



Review

Functional Mesoporous Silica Nanocomposites: Biomedical applications and Biosafety.

Rafael R. Castillo and María Vallet-Regí*

Dpto. Química en Ciencias Farmacéuticas. Facultad de Farmacia, Universidad Complutense de Madrid. Plaza Ramón y Cajal s/n, 28040, Madrid, Spain.

Centro de Investigación Biomédica en Red –CIBER–

Instituto de Investigación Sanitaria Hospital 12 de Octubre –imas12–

Corresponding author: vallet@ucm.es

Abstract: The rise and development of nanotechnology has permitted to create of a wide number of systems able to accomplish new and advantageous features to treat cancer. However in many cases, the lone application of those new nanotherapeutics has proven not to be enough to achieve acceptable therapeutic efficacies. Hence, to avoid these limitations, the scientific community has been embarked on the development of single formulations capable of combining functionalities. Among all possible components, silica –either solid or mesoporous–, has become of importance as connecting and coating material for those new-generation therapeutic nanodevices. In the present review there are visited the most recent examples of fully-inorganic silica-based functional composites, paying especial attention to those with potential biomedical applicability. Additionally, there will be given some highlights about their possible biosafety issues based on their chemical composition.

Keywords: Mesoporous Silica; Magnetic; Photothermal; Photodynamic; Combination therapy; Drug Delivery

1. Introduction

The unstoppable advance of nanotechnology during the last decades has led to the development of a large number of nanomaterials with great therapeutic potential. Focusing on the treatment of cancer, the biomedical area with greatest penetration of nanometric based therapies, is possible to find a large number of materials suitable to treat an also large number of pathologies [1,2]. For example magnetic [3,4] and plasmonic materials [5–7] could be remotely excited with magnetic fields and light respectively to produce a thermal response capable of inducing cell apoptosis. Similarly, photodynamic chemical sensitizers [7] can generate Reactive Oxygen Species (ROS) inducing cell death throughout the oxidative stress pathway. Although these alternative therapies can improve the prognosis of the disease when employed as adjuvants, the truth is that chemotherapy remains as the reference treatment.

Fortunately, delivery of chemotherapeutics have been also evolved, allowing the development of nanoencapsulated drug formulations able to improve the pharmacological profile of free drugs. In the clinic, liposomes [8,9] stand out, distantly followed by drug-protein hybrids and polymeric particles [1]. Nonetheless mesoporous silica (MS) based materials are slowly beginning to gain relevance because two unique properties: their well-established drug delivery properties [10,11] and their versatility to create high performing hybrid materials, which is the purpose of the present review. The classic features of Mesoporous Silica Nanoparticles (MSNs), related to their porous and robust structure, have given them notoriety in the academic field as drug delivery systems [12]. But in the last decade, the implementation of silica technology into other nanomaterials allowed the successful combination of several components in single nanometric entities. This, apart from an academic interest, has also aroused a certain clinical interest, since the additional nanosystems'

functionality could be successfully integrated with the well-known drug load capabilities of the MS. Therefore, the multiple integration of features in single entities could be a pipe dream and its definitive weakness, since in the same way that raw nanomaterials have certain security issues and limitations, those are transferred to composite materials. In this review we will focus on the development of hybrid inorganic-silica materials with multiple features with applicability in nanomedicine and cancer treatment. Moreover, there will be discussed the additional features and known safety issues related to each functional silica-containing composites; however, as the MS will be common to all materials, we will begin with the biosafety aspects of silica. Apart from MS, there also have been reported other multifunctional devices based on different nanoplateforms [13–16].

Bulk silica is widely present in food additives and cosmetic products, which indicates low toxicity in the body; in general, silica is catalogued as “Generally Recognized as Safe” by the FDA (US Food and Drug administration, ID Code: 14808-60-7). Despite the demonstrated biocompatibility of bulk silica, when any chemical species is prepared as a nanomaterial, new risks, limitations and safety issues appear as a consequence of their tiny size. For example, the intimate interaction between particles and cells that allow nanomaterials to be assimilated by tumor cells, could generate unexpected side effects in healthy organs if they are accumulated or induce sensitization [17].

Despite these limitations, MSNs are considered too as safe materials for biomedical applications [18–20] as they suffer from slow hydrolysis in aqueous media [21–23] which may last up to weeks depending on pore conformation and functionalization. For raw MSNs matrix degradation is of capital phenomenon to properly determine the release kinetics; although in functional composites and modified silica this parameter is harder to control as more parameters apply and much less information is available.

Apart from the degradability and the possibility to be excreted (Figure 1), there are other parameters and effects that should be accounted on MSNs in order to prepare them as nanomedical devices [23,24]. Size [25], shape [26–28], pore volume [29] and surface functionalization are also capital aspects. Regarding morphology, it is accepted that MSNs between 100 and 200 nm are the best performing particles; as those (1) avoid fast clearance [20] and acute toxicity [30,31] associated to small particles and (2) avoid aggregation on physiological fluids, blood capillaries and alveoli [32] associated to bigger particles. Moreover, rod-like particles seem to behave better than spherical ones thanks to the fact that multivalent interactions with membranes are easier [26,33].

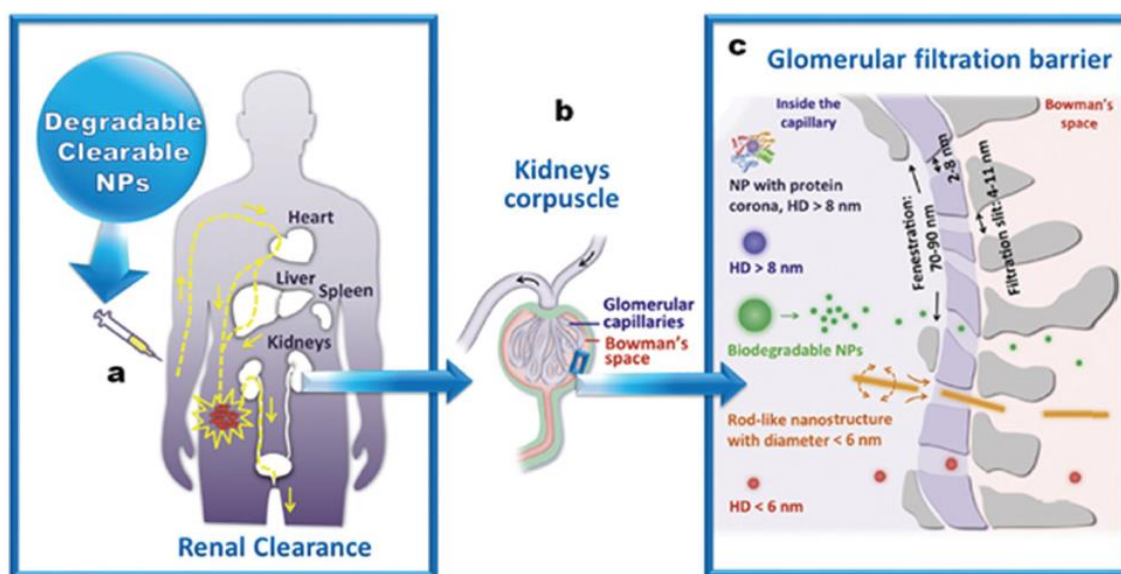


Figure 1. (a): Major organs involved in the biodistribution of nanoparticles. (b and c): Schematic glomerular clearance possibilities depending on the biodegradability and size of nanoparticles. Adapted from reference [34] with permission.

Regardless of the morphology, the superficial modification of the MSNs plays a fundamental role in their efficacy and safety. First of all, it must be borne in mind that the use of the EPR effect alone, although could improve the behavior of the free drugs, is not often enough to give rise to personalized therapies and to improve the efficiency of available treatments. For this reason, there have been created a number of nanosystems able to increase the specificity towards certain cell populations. In this sense, a multitude of systems in which silica is coupled with recognition elements such as antibodies, aptamers and other bioactive fragments have been described [35–37]. On the other hand, it is also important to account that exogenous nanoparticles undergo a deposition of serum proteins as a result of the interaction with the immune system. This process called opsonization, leads to a strong surface modification -protein corona- [38,39] which produce the disruption of particles' recognition abilities and finally to their elimination. Fortunately, opsonization could be mitigated by including highly hydrophilic polymers or fragments such as polyethyleneglycol [40,41] or zwitterion structures able to create strong hydration layers onto the surface [42,43].

Besides surface modification, it is also important to consider that connections between components require from additional in-between layers. One of the most common substances for such purposes is dense silica, usually employed in thicknesses around several nanometers. The role of this intermediate layer usually goes beyond providing chemical inertness and magneto-optical transparency. It also permits to physically separate both components, avoiding physicochemical processes like dissolution or passivation of the internal core and the quenching of fluorescent-labelled composites. Moreover, it also permits the generation of additional mesoporous layers without adding complexity to the system. It is also important to account that these dense silica layers have demonstrated additional features, some of them reviewed below, as increased photothermal stability of cores or the possibility to tune relaxativity of contrast agents in Magnetic Resonance Imaging [44-46].

In view of all these aspects, to currently classify MSNs as suitable devices for biomedical applications, they must comply with series of morphology and surface modification requirements aimed at minimizing the immune response –stealth– and enhancing tissue/cell recognition –targeting–. As expected, all these features must be also complied if silica-containing inorganic composites are intended for biomedical applications.

2. Inorganic-Mesoporous Silica nanocomposites with magnetic response.

2.1. Magnetic materials in the clinic

The use of magnetic nanomaterials is one of the most active research areas in biomedical research [4447], as proven by the large number of these nanosystems ongoing clinical trials [2]. Usually, those magnetic materials consist on crystalline iron oxides whose surface has been engineered to avoid agglomeration and accelerated dissolution [4548]. Among known nanometric magnetic materials Superparamagnetic Iron Oxide Nanoparticles (SPIONs) are by far the most developed systems [4649]. In this way SPIONs are magnetized in the presence of external magnetic fields, while they do not show such behavior in its absence. Moreover, SPIONs show a diverging behavior depending on the external magnetic field. Hence, if constant magnetic fields are applied (permanent magnet), magnetized SPIONs could be remotely guided towards the magnet; while if under alternating magnetic fields, SPIONs suffer from magnetization shifts. If this oscillation is powerful enough, the continuous reorientation of the magnetization will generate a magnetic resistance which would be thermally dissipated. This effect, when employed on living systems, lead to heat-induced apoptosis known as magnetic hyperthermia [4750]. Additionally, SPIONs have broad applicability as contrast agents for Magnetic Resonance Imaging (MRI) [4851,52,49] since they could be easily modified to tune their affinity to cells or tissues.

Regarding the biosafety of clinically interesting SPIONs is important to remark that iron oxide crystals smaller than 20 nm, suffer from quick clearance but outstanding biocompatibility [5053] and require from surface coating to obtain higher circulation times and immune stealthing. Among all

coatings, dextran, starch, or PEG polymers are the most employed; being –the low molecular weight dextran the most recurrent on clinical trials [2,50].

2.2. Iron Oxide-Mesoporous Silica Nanocomposites (IOMSNs) as drug delivery agents.

The coating of raw SPIONs ~~with silica~~ is of interest because it allows to increase time-stability by preventing its dissolution and undesired aggregation processes, among other important features. Among all SPION-Silica hybrid species, the mesoporous ones have special relevance as allow to develop Magnetic Drug Delivery Systems (MDDS). Nevertheless this coating also may induce use limitations, as a MS shell may produce thermal insulation of the magnetic core [5454]. This effect, although with little relevance in MRI and magnetic guidance, needs to be accounted if Magnetothermal-chemotherapy (MTCT) is intended [5255]. Despite the improved *in vivo* stability provided by the silica coating of IOMSNs, this outer shell must be also chemically modified to avoid the interaction with adhesive proteins of the immune system [5356]. This could be achieved by any of the conventional coating procedures known for silica: polyethyleneglycol, [57,5854,55] small targeting elements, functional polymers, zwitterions, small-interfering RNAs (siRNAs) deposition and coating with membranes; although none of these materials have still reached clinical studies as far as we know (Figure 2). Among all surface coatings developed so far, PEG is by far the most recurrent component for SPIONs and IOMSNs [5659]. However, if such MDDS are not properly targeted, they would show a limited cell uptake and incremented off-target accumulation which may lead to severe problems of misplaced heating. To avoid this, many efforts have been devoted to the development of PEG-modified polymers able to efficiently target cells.

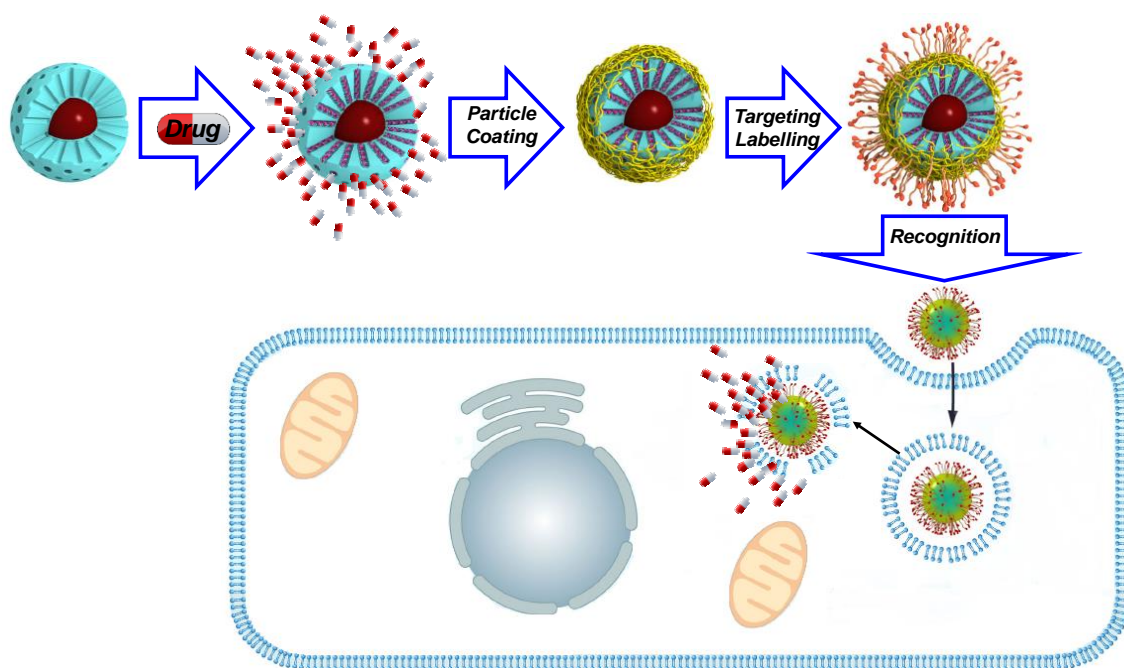


Figure 2. Typical strategy employed for the preparation of drug-loaded, polymer-coated, targeted IOMSNs reviewed herein.

Besides PEG-based polymers, there are many other interesting examples of polymer coated IOMSNs composites in the literature. For example, Zhang and coworkers employed a poly-dopamine pH-sensitive shell to retain Doxorubicin (DOX) within the mesopores [5760]. Additionally, this system was functionalized with a folate-modified PEG to provide targeting towards HeLa breast cancer cells. The efficacy of this coating was assessed using cell viability studies, which demonstrated high survival rates *in vitro* when the coating was present. The folate targeting employed permitted to reach high values of tumor accumulation without significant accumulation onto major organs. In another example by Hanagata there was designed a thermosensitive polymeric shell for IOMSNs [5861]. Herein, the chosen *N*-isopropylacrylamide

(NIPAM) containing polymer had the ability to change its conformation from globular to expanded when heated. With this system the authors could efficiently deliver DOX in combination with magnetic induced heating. This system proved to have an enhanced apoptotic effect on HeLa cells. Moreover, Guisasola *et al.* [5962] employed an equivalent device *in vivo*. On this work it could be seen that combination of hyperthermia and chemotherapy led to tumor growth reversion, demonstrating the potential of MTCT.

Other common polymer employed on MDDS is polyethyleneimine. This is widely employed because of its cationic character that permits to bridge together negatively charged moieties like particles and nucleic acids. For example, Lee and coworkers developed a multilayered Zn-doped IOMSNs magnetic device able to successfully deliver DOX and the lethal-7a (let-7a) micro RNA (miRNA) able to disrupt Heat-Shock Protein expression. To do so the authors prepared negatively charged, phosphonate IOMSNs which were coated with PEI, (10 kDa) polymer. Then onto it was deposited the miRNA and a RGD modified PEI layer [6963]. The resulting RGD-targeted cationic assembly provided enhanced internalization on MDA-MB-231 breast cancer cells. This MDDS provided a satisfactory tumor volume reduction although magnetic hyperthermia was not employed.

Although polymer coating of raw and hybrid MSNs enables outstanding retention of drugs within the mesopores, it is necessary to account that those polymers usually have associated severe drawbacks due to their limited degradability and/or intrinsic toxicity. For example PEI polymers larger than 25 kDa [6464] are known to highly destabilize cell membranes promoting apoptosis, unreacted NIPAM monomers are highly toxic [6265], while PEG polymers are generating a growing immunity [63,6466,67] due to their ubiquity in pharmaceuticals. For these reasons, many research groups are trying to avoid those issues by moving towards the use of more convenient biogenic elements to develop targeting and gating. For example, Popova *et al.* employed chitosan and alginate polymers to make a multilayer coating of sulfonate modified IOMSNs [6568]. This double coating is based on the electrostatic interaction of the cationic chitosan with both anionic IOMSNs and the alginate layer. This particular assembly permitted to load two different drugs mitoxantrone, within the mesopores, and prednisolone in between the chitosan-alginate layer. Other example was reported by Sinha *et al.* who deposited dextran onto boronic acid modified IOMSNs [6669]. This system proved to be sensitive to glucose, which was able to displace the dextran chains from the boronic acid. This system proved to successfully deliver Camptothecin on HeLa breast cancer cells thanks to the presence of folic acid as targeting agent. Unfortunately, the potential of this device was not fully tested as the combined apoptotic effect of MTCT was not addressed. Glycopolymers have been also employed for coating IOMSNs; for example, Lactobionic-2-aminoethyl methacrylate and 3-(Methacryloxy)-propyltrimethoxysilane were co-polymerized onto IOMSNs for drug delivery [6770]. In this case, the pH-sensitive polymeric shell was able to retain DOX, unless a lysosomal escape occurred. Although the potential of MTCT was not addressed, the authors determined the fate of these MDDS in a murine model employing MRI detection.

In order to enhance composites' performance, other exploited approach is the modification of the surface with targeting elements. In an interesting contribution by Gao *et al.*, folic acid was employed as coating for the silica layer [6871] to develop a targeted system able to exert MTCT. On this system, as there was not included a thermo-responsive nanogate, so the DOX release showed the same pattern in presence or absence of the alternating magnetic field. As expected, the application of a simultaneous MTCT showed a synergistic apoptotic effect *in vitro* on human MCF-7 breast cancer cells. Similarly, a recent paper by Kariduraganavar and coworkers employed IOMSNs with transferrin on its surface to address U87 human glioblastoma cells [6972]. Moreover, the authors employed a Blood-Brain Barrier model to demonstrate that these nanosystems are able to cross this barrier.

Apart from biogenic moieties, many functional modifications have been also included onto IOMSNs. For example Portilho *et al.* designed a theranostic system using a surface ⁹⁹Tc-containing ligand for SPECT imaging with dacarbazine for the detection and treatment of melanoma [7073]. Other synthetic approach, aimed at improving the circulation time is the use of zwitterion elements

on the surface. Those molecules with perfectly balanced but separated charges are known to create a strong hydration layer that prevents protein adhesion [7474]. In a nice example by Sánchez-Salcedo *et al.* phosphonate capped IOMSNs were coated with a low-weight cross-linked PEI onto which was grafted a zwitterion phosphorylcholine fragment [7275]. Moreover, on this nanosystem the remainder free amino groups from PEI were balanced with a siRNA to achieve multimodal magnetically induced MTCT plus gene silencing. For the time being this system has only been partially tested *in vitro* with promising results on Ovar8 ovarian cancer cell line.

In addition to polymers and small molecules other promising coating for IOMSNs are lipid bilayers [7376], similarly as the so-called protocells. In a pioneering example by Mattingly *et al.* there was employed a cationic lipid shell to entrap DOX within IOMSNs [7477]; unfortunately, this magnetic protocell led to a relevant death rates on tested cells due to the cationic lipid bilayer employed. Nevertheless, this example set the basis for Sen and coworkers to design a phospholipid coated system to deliver DOX to MCF-7 and U87 cell lines [7578]. In this case the authors obtained an outstanding biocompatibility unless drugs or magnetic hyperthermia were applied. More recent examples deepened in the potential of this capping strategy, as elegantly demonstrated by Li and coworkers, who cloaked their nanocomposite with red blood cell membranes [7679] to obtain excellent biocompatibilities and circulation times (Figure 3).

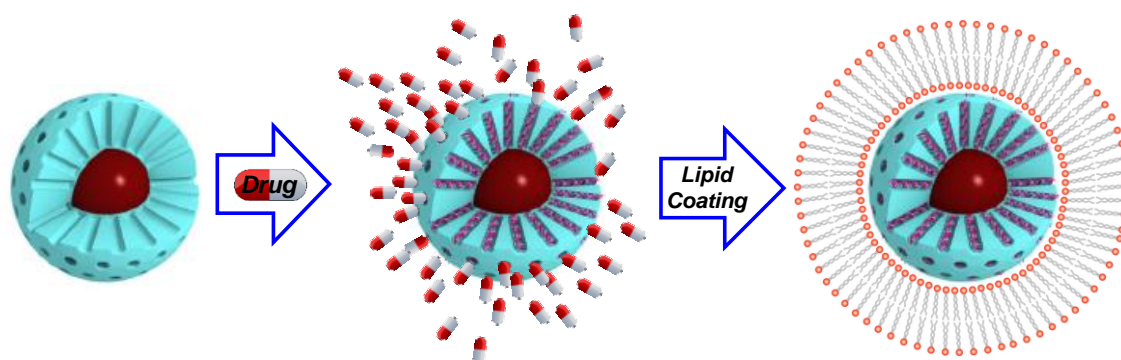


Figure 3. Multifunctional protocells arise from the coating of Mesoporous silica-based composites with lipid bilayers.

Besides organic and biological coatings, other interesting systems with promising behavior have been also developed. For instance, Liu *et al.*, coated Folate-targeted IOMSNs with a fully biocompatible CaCO_3 as acid-cleavable gatekeeper for Daunorubicin delivery [7780]. This strategy, although profits from a simple and effective end-cap coating method based on the precipitation of CaCO_3 from CaCl_2 and Na_2CO_3 , seems to affect the targeting capabilities of the complete system as suggested by the loss of preferential uptake.

2.3. Magnetic Composites with applications in Nuclear Magnetic Imaging (MRI).

The use of superparamagnetic materials in MRI is of great importance to achieve better contrast between tissues [4851]. In the case of transversal magnetization imaging (T_2 weighted MRI, employed mainly for low-fat highly hydrated tissues) SPIONs are known to shorten spin-spin relaxation time of water and to provide better contrast in lean tissues such as liver, spleen and kidneys. On the other hand, longitudinal magnetization imaging (T_1 weighted MRI, more useful to visualize tissues with high fat or low water contents) is improved when paramagnetic cations Mn^{2+} , Gd^{3+} and mainly Fe^{3+} are used as sensitizers.

Unlike sensitizers exclusively designed for MRI, nanodevices containing metal and silica oxides are gaining interest as they can be employed for simultaneous diagnosis and therapy –theranosis– [78,7981,82]. However, the sensitivity provided by IOMSNs for T_2 MRI is usually lower than those of SPIONs. This effect, caused by the shielding effect of silica, could be reversed if metal oxides are in the outermost layer of the composite. Moreover, the sensitivity provided by IOMSNs for T_2 -MRI is usually higher than those obtained for SPIONs, as recurrently demonstrated on the literature [83,84].

This effect could be also obtained by increasing the number of sensitizers throughout strategies that employ a greater number of metal oxides, which would be generally placed at the outermost layer of the composite. Those Mesoporous Silica-Metal Oxide Nanocomposites (MSMONs) show promising properties because of the higher metal loads achieved and the outstanding biocompatibility of components. Nonetheless, this approach has also limitations, as coating nanoparticles must be functionalized too to avoid all undesired aggregation processes, opsonization, off-target uptake and/or immune response.

The coating of MSNs with SPIONs was first reported by Victor Lin's group who designed a stimuli-responsive delivery system using silica nanorods [8085]. Although this responsive composite was intended as a proof of concept, the authors clearly outlined a future biomedical approach as they employed a redox-cleavable linker sensitive to biogenic compounds. More recently, Hyeon and coworkers developed PEG-coated MSMONs employing chemical ligation between amino capped MSNs and bromoalkyl-modified SPIONs [8186]. To do so, PEGylated the outer surface following a two-step methodology: (1) reacting the amino groups with a succinimidyl carboxylate PEG which was then (2) functionalized with previously PEGylated SPIONs. This model exemplifies the difficulty of preparing those MSMONs, which apart to need from two different stealthing agents, must be carefully synthesized to avoid massive aggregation between particles.

With the previous design in mind and with the purpose of developing a synchronous *T1* MRI contrast agent Zou and coworkers developed a MSMONs employing Ultra-small Manganese Oxide Nanoparticles to cap mesopores [8287]. Those caps could quickly dissolve under weakly acidic and release Mn^{+2} to enable *T1* weighted imaging. Moreover, the authors employed DOX within the pores to have an additional therapeutic effect (Figure 4). Employing a similar strategy Huang *et al.* designed a system in which MSNs were doped with Fe^{+3} and loaded with DOX [8388]. This device proved to release ferric cations together with DOX when reached mild-acidic environments, accounting its use as a theranostic platform too. Moreover, although not reported, these DOX-loaded, metal-doped MSNs are supposed to be fully biodegradable as only Si, Mn and Fe oxides are employed on their synthesis (Figure 4).

Regarding Gd, the most widely employed contrast agent for MRI, there have been also reported a broad number of systems. Like in previous examples, the strongly paramagnetic Gd^{+3} ions could be either located onto the surface of MSNs throughout known chelants, doped within the porous silica matrix, or even as a core-shell structure. The first approach, chelation throughout ligands, proved to be suitable for the generation of MSNs with contrast properties for MRI [89,90]. Along this line, it is important to remark the work by Davis and coworkers, who determined that surface location of Gd-chelates led to better contrast and sensitivity [91]. Unfortunately, this approach has a severe drawback, as surface modification is highly limited and complex due to the presence of Gd-chelates.

For this reason new strategies have been developed for the incorporation of Gd into functional nanosystems. One of those possibilities is doping the silica matrix, which liberates the surface for further functionalization. However, a poor signal-to-noise ratio arises as a consequence of placing Gd in a mismatched crystallographic matrix. Hence, to overcome this issue two strategies that employ compact Gd-matrices has been reported. The first, in which the Gd occupies the core and the silica the shell, has the advantage of enabling multimodal detection throughout *T1* weighted MRI and NIR-emitting persistent luminescence. Moreover, such approach allow to further modify the MS layer with all the developed targeting and stealthing technology, as elegantly demonstrated by Yu and Chen groups [92,93]. The other possibility for obtaining solid Gd-containing matrices is based on the construction of Gd-shells [94]; although this strategy does not profit from the advantages associated to mesoporous silica coatings.

The previous examples use MSNs to, upon thermal treatment, dope the silica matrix. This strategy, although suitable for the release of paramagnetic cations, does not enhance the SPION-mediated *T2* imaging. To solve this problem, Miao and coworkers devised a strategy in which MSNs were coated with core-shell SPIONs@MnO nanoparticles [8495]. This system could be disassembled when either (1) pH is below 5, (2) Glutathione (GSH) is overexpressed or (3) ROS are

above normal values. As expected, such system showed negligible effect on the viability unless Camptothecin was loaded, thus demonstrating an outstanding biocompatibility.

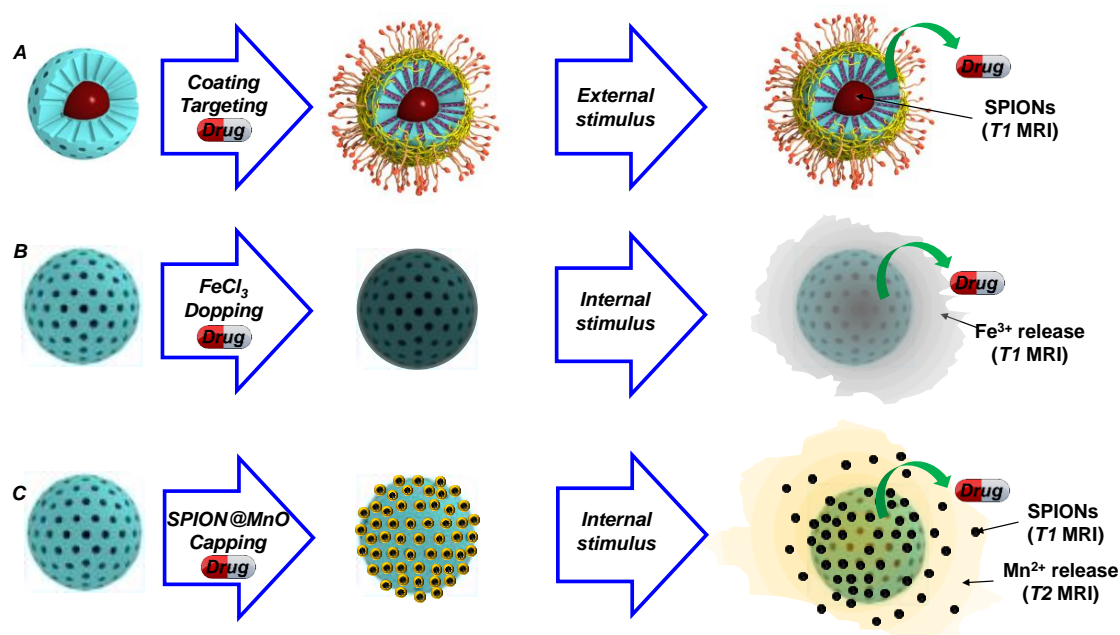


Figure 4. Possible strategies for the preparation of Mesoporous silica-containing composites for MRI detection. (a) SPIONs contained in IOMSNs enable *T1* weighted MRI while the outer mesoporous silica shell facilitates the development of hyperthermia-triggered systems. (b) Doping the silica matrix with acidic cleavable contrast cations for *T1* weighted MRI. (c) Capping mesopores with doped SPIONs for favoring acidic release of *T1* (SPIONs) and *T2* (Mn²⁺) contrast agents.

Regarding the biosafety of those species, there should be accounted that capping nanoparticles must comply with all the premises made at the beginning of this revision. They must have an adequate surface functionalization to provide enough colloidal stability and to avoid the action of the immune system. Moreover, nanocaps must be either efficiently cleared or biodegraded; although in any case, use of small nanoparticles for capping purposes clearly aid in their final elimination. Regarding the cores, the use of ionic species (such as iron oxides reviewed herein or CuS and UCNs reviewed below) do not seem to be a problem regarding bioaccumulation as they degrade; although they may suffer from acute toxicity issues. But the use of non-degradable species (as Au) must be carefully addressed, as will be discussed along the following lines.

2.4. Remote Homing of Magnetic Mesoporous Silica nanocomposites

One of the most acclaimed applications of MDDS is the possibility of achieving magnetic guidance; although for magnetic silica composites is difficult to find successful examples. One of those is the model reported by Lee, which profited from a facilitated *in vitro* magnetic transfection to increase the apoptotic effect induced by hyperthermia plus DOX and let-7a miRNA co-delivery into glioblastoma multiforme cancer cells [6063].

However, when magnetic guidance is intended *in vivo*, the round shaped composites do not seem to be the choice option. For these purposes, bifunctional *nanobullets* consisting of a Fe₃O₄ magnetic head attached to a mesoporous silica tail seem to be a better option according to the results published by Dong and coworkers [85–8796–98]. On their first formulation, the authors employed Fe₃O₄ magnetic particles produced throughout high temperature hydrolysis with poly(acrylic acid) as surfactant. Then, onto those there were prepared MS rods upon a controlled addition of the silica precursor. The resulting MS tail was functionalized with amino groups onto which PEG was grafted, obtaining the desired *Janus Iron Oxide Mesoporous Silica Nanobullets* [8596]. This system was deeply

tested *in vitro* demonstrating a very nice biocompatibility together with evidences of energy dependent clathrin uptake.

In vivo bioaccumulation of this system on HepG2 tumor-bearing mice demonstrated a preferred accumulation on the spleen. However, when magnetically targeted, the liver and the hepatic tumor were the tissues with highest accumulation, proving an effective magnetic guidance. Unluckily, despite the obtained tumor accumulation, the use of these *nanobullets* as DOX delivery agents did not improve the use of free DOX. To overcome this negative result, in a subsequent investigation the authors implemented the system by using a prodrug (Ganciclovir) loaded in the mesopores plus the herpes simplex virus thymidine kinase (prodrug activator) outside the pores. To retain the enzyme within the carrier the system was finally coated with a poly(L-lysine)-poly(ethylene glycol) layer grafted onto the carboxylate-modified *nanobullets* throughout amide coupling [8697]. Both *in vivo* and *in vitro* studies showed that combined guidance and MTCT permitted to significantly reduce the viability of cells and tumor sizes. More recently, these authors kept on studying the possibilities of this bullet-like MDDS, in this case to deliver curcumin to HepG2 cells [8798]. The result of combining these three effects: magnetic induced delivery, hyperthermia and curcumin delivery was an effective tumor reduction; which was not obtained when any of these three proapoptotic factors were absent.

In addition to it, in these works the authors tackled too four different but important aspects of MDDS: (1) they compared the round-shaped (isotropic) core-shell disposition against the *nanobullet* (anisotropic) configuration, finding higher drug loading and faster release on the *nanobullets*; (2) the bullet-like materials demonstrated better magnetic guidance and hyperthermia due to their non-insulated magnetic head; (3) *nanobullets* provided an enhanced gene delivery when compared to the core-shell IOMSNs and finally (4) proved that the use of hyperthermia in combination with the gene suicide therapy led to a significant tumor growth control.

In summary, Dong's group have demonstrated the versatility of their *nanobullets* platform for multifunctional nanosystems, as they successfully accomplished: remote guidance, drug delivery, hyperthermia and MRI. Moreover, the use of stealth PEG-based coatings, permitted to reduce aggregation and immune system clearance thus favoring diffusion and increasing the therapeutic effect. As a drawback, the authors did not address yet the use of efficiently targeted *nanobullets* which might improve the efficacy of the magnetic-induced accumulation (Figure 5).

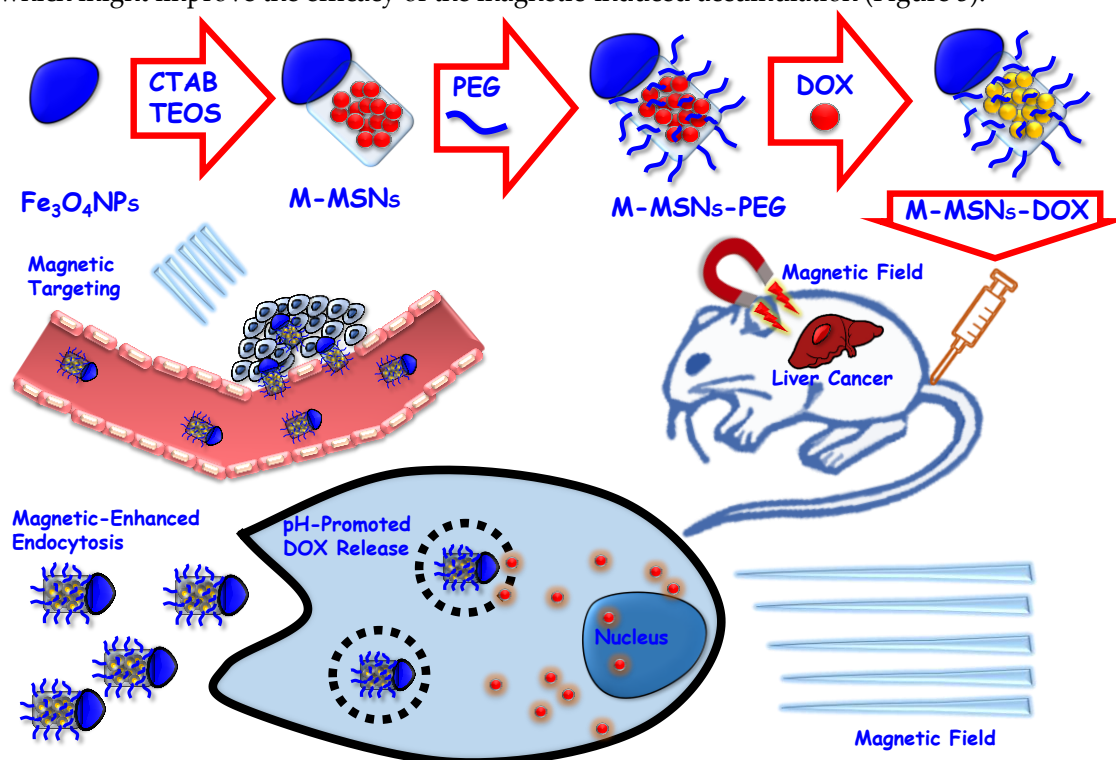


Figure 5. Janus-nanobullets employed for magnetic-targeted drug delivery.

2.5. Magnetic Based Nano- and Biosensors

Magnetic materials have in nanosensors another important field of development. One of the most promising approaches, although restricted to *in vitro* assays, is Magnetic Relaxation Switching [8899]. This strategy profits from the increase of T_2 transversal relaxation time suffered by SPIONs when aggregated; which if caused by an analyte, would enable to develop MRI [89100] or relaxometry [90101] based-sensors. However, this approach is not suitable for most of systems described herein as the MS layer do not permit such close contact aggregation.

In addition to them, magnetic nanomaterials have been also described as lipophilic-sample enrichment systems; which are based on the interaction of hydrophobic-coated SPIONs with lipophilic substances. Please refer to the following reviews to deepen in the uses of hydrophobic (C8 to C18 chains, Carbon nanotubes, Graphene, Surfactants, Polymers, etc.) modified IOMSNs [91,92102,103]. From a safety point of view, although those nanosystems are able to adsorb substantial amounts of highly lipophilic proteins and analytes; the nature of those surface modifications make these systems extremely incompatible with living organisms and restrict their use only for *in vitro* purposes.

2.6. Magnetic biostimulators

Another important aspect of magnetic therapy is the remote induction of latent behaviors in treated cells. Among them, the most exploited is hyperthermia, an apoptosis inductor; however new interesting possibilities for other bone diseases have been also reported [93104]. Along this line, Deng and coworkers, employed IOMSNs arrays to suppress osteoclast differentiation [94105]. This effect opened the way to develop novel therapies for osteoporosis; mainly when in combination with the antiresorptive effect of zoledronic acid. For preparing such arrays the authors prepared silica coated SPIONs. Then, those were aligned to an external magnetic field, maintaining the alignment thanks to a magnetic dipolar interaction, then it was possible to coat the array with an additional mesoporous layer. The resulting linear, stable mesostructures could be prepared in up to 15 μm . The considerable length showed by this particular composite material permitted to remotely induce shear forces which proved to inhibit osteoclasts differentiation in concentrations above of 62.5 ng/mL. However, despite the significant advance could be the remote disruption of the resorptive pathway for osteoporosis, the biosafety of this material could be questioned; first the enormous (from 1 to 15 μm) length might induce severe embolisms by composites' aggregation, mainly after considering that the outer silica layer is not treated with stealthing agents. But also, the delivery of those materials towards the target could be problematic due to their complicated delivery to the bone. Notwithstanding all their limitations, the evolution of those IOMSNs' nanochains is of an extraordinary interest, as it described the first remotely-triggered example for treating osteoporosis.

3. Inorganic-Mesoporous Silica nanocomposites responsive to light.

3.1. Nanomaterials with thermochemical response: Photothermal and Photodynamic effects.

It is well known that certain materials are able to interact with light producing physical effects different from refraction, absorption and dispersion. In some cases, the light stimulation may produce either a thermal or an electronic excitation, which could be of interest for biomedical applications. In this way, if the resulting effect is thermal, it will be considered as a photothermal effect (PTE) [95106], while if it is a light-driven chemical excitation, we would talk about Photodynamic Effect (PDE) [107,10896,97]. This second effect is originated when the electronic excitation is relaxed by an energy-transfer to surrounding molecules, leading to ROS -that may undergo oxidative stress in living systems. The third possibility considered herein is luminescence, which will be reviewed below. All those possibilities have proved their feasibility for biomedical applications thank to a number of highly interesting contributions; although in some cases their use is not exactly innocuous.

The Photothermal Effect can be achieved either with organic or inorganic materials. The organic ones include the use of carbon allotropes [98109] (graphene, nanotubes, etc.) and conjugated polymeric materials [99110]; whereas among the inorganics, the greatest exponent are those derived from Au [5,111400]. The common problem to all these materials is their enormous facility to accumulate in living organisms, as they are not easily biodegraded. This can lead to both long-term toxic effects and latent but unwanted, off-target photothermal effects. For this reason, it is of vital importance to use those photoactive species in sizes that allow an efficient excretion and in very small quantities. Fortunately, the development of composite materials with a MS coating, allow to tune the overall size avoiding their aggregation. Moreover, the use of silica for PTE is highly convenient because of its transparency in Near Infrared (NIR); although produces thermal insulation of the photothermal core and thus lower responses. Besides therapeutic PTE, NIR excitation could be also employed for on-demand drug delivery purposes, for more information on this topic, please refer to reference [404112].

The PDE occurs when the sensitizer is able to gather photons and transfer them to other reactive chemical species. Photosensitizers (PS) could be either of organic and organometallic nature: phenothiazinium cations, porphyrins, and phthalocyanines [402,403113,114], but also of inorganic nature. Among those, there have been reported examples of particles with PDE employing Fe_3O_4 [404115], TiO_2 [405116] and ZnO [406,407117,118] nanoparticles. Moreover, PDE is also common for Au and CuS nanoparticles, as a side relaxation pathway complementary to PTE. The use of PDE with Fe, Ti and Zn oxides is based on UV irradiation and has severe limitations for living systems. Fortunately, as will be discussed below, the use of UV radiation can be avoided by using composite materials containing upconversion particles, which are able gather photons from low energy radiation and convert them onto UV radiation able to excite photosensitizers and thus create the desired ROS. The main advantage of this strategy is the use of a harmless light source and the extremely localized generation of UV light, which only occurs where upconversion nanoparticles are present. Those two aspects enhance the biosafety of composites for PDE, although only if the PS is eliminable. For more information about PDE, please check the outstanding review authored by Lucky, Soo and Zhang [97108].

Besides their potential, non-degradable photosensitizers have severe side effects such as latent sensitivity, off-target accumulation and chronic toxicity. For this reason, the scientific community has been interested on the development of safer alternatives. Relevant examples for PTE induction could be achieved with degradable CuS [408,409119,120] and Fe_3O_4 [440121,122,144] crystals, which due to its ionic nature could be fully biodegraded. Unfortunately, up to our knowledge, there are no low risk photosensitizer alternatives for PDE. Their side-toxicity or latent reactivity must be always accounted in biomedical applications. An in-depth discussion of the advances that provide the combination of photodynamic or photothermal therapies together with anticancer drugs could be found in a previous review by us. Interested readers, please check reference [5255] for details.

3.2. Inorganic Mesoporous Silica Nanocomposites for Photothermal Therapy.

As previously introduced the most typical materials for PTE are Au species, and among them Gold Nanorods (GNRs). Nevertheless, they show two important limitations: the impossibility to be degraded and the presence of remainder surface surfactant CTAB hauled from its synthesis. Fortunately, the toxic cationic surfactant issue could be mitigated by coating the GNRs with a MS matrix. The resulting Mesoporous Silica Coated Gold Nanorods (MSGNRs) provide a stable coating that prevents aggregation and morphology shifts while preserves its plasmonic properties and thermal response (Figure 6). In a pioneering example Wu, Chen and coworkers were the first to deliver DOX with MSGNRs, [442123] proving that the simultaneous photothermal-chemotherapy (PTCT) provided an enhanced apoptotic effect. Inspired by the potential of PTCT, many other examples were reported in the following years profiting from the facile surface functionalization of the MS outer layer. Those modifications could be aimed at modifying the release profile of loaded drugs or to turn the systems into actively targeted devices.

Regarding the drug release modification, there could be found many examples in the literature. For example, the system designed by Lin, Qu and coworkers employed a pH-sensitive imine bonds to connect DOX and MS, obtaining a pH-driven release [443124]. On the other hand, there have been also reported targeted systems. In one of the first examples Liu et al. reported the surface modification of MSGNRs with a PEG polymer modified with a targeting tLip-1 peptide selective to the Neurophilin, a protein present in many cancer cell lines [444125].

Capped systems have been also object of study, although in this case the interest is shifted to thermally responsive systems more than for PTCT. In one of the previous examples Duget and coworkers have coated folate-targeted MSGNRs with a low-temperature (39°C) melting biocompatible component [445126]. The 1-tetradecanol employed permitted to effectively coat the outer MS layer, thus allowing the retention of small molecules within the mesopores. However, when the system was exposed to NIR light and heated, the gatekeeper melted, and the drug could be released. In this case the authors did not pay attention to possible sensitivities to the 1-tetradecanol release, which may have disrupted the normal function of membranes and enhanced the overall apoptotic effect. On this same topic, our group developed a reversible nanosystem in which pore gating is accomplished by a NIPAM-based thermo-sensitive polymer [446127]. In order to get the appropriate functionalization and an adequate transition temperature a hydroxyl-containing monomer was included. Onto it there could be anchored and a bifunctional PEG that allowed to incorporate the melanoma-targeting NAPamide peptide. The system, evaluated *in vitro*, proved to be selectively accumulated into melanoma cells, producing the expected increase of cell death when combined PTCT was exerted.

Apart from AuNRs, there are other Au species that show plasmonic properties. Among them, nanostars and nanoshells are the most promising (Figure 6). As expected, there have been successfully prepared hybrid species with MS. For a review dealing with Au@MS hybrid species, please check reference [447128]. Although the use of Gold Nanostars (GNSts) in combination with MS is very recent, there have been reported several examples with comparable efficiency to those obtained for the MSGNRs. In the first reported example using GNSts-MS hybrids, Zhang *et al.* designed a *Janus*-Au-Silica composite which was employed to successfully deliver DOX to HepG2 cancer cells [448129]. Moreover, the *Janus* disposition of Au and Silica permitted to functionalize both subunits differently: Au was capped with a stealth PEG polymer while the silica moiety was decorated with lactobionic acid to gain in stability, biocompatibility, blood circulation time, and targeting towards cells bearing asialoglycoprotein receptors. Oppositely to the following examples, which employ already shaped GNSts, in this example the nanostar was prepared after the partial coating of an AuNP with MS. More recent examples dealing with GNSts could be on the literature. For example Martínez-Máñez and coworkers developed an AuNSt@MS system coated with paraffin for DOX delivery [449130]; while Raghavan *et al.*, employed GNSts@MS for theranostic simultaneous PTE and photoacoustic detection [420131]. In this last contribution the authors showed interesting results when a MS coated the nanostar: (1) a red-shift in the plasmon wavelength and (2) an enhanced photoacoustic effect.

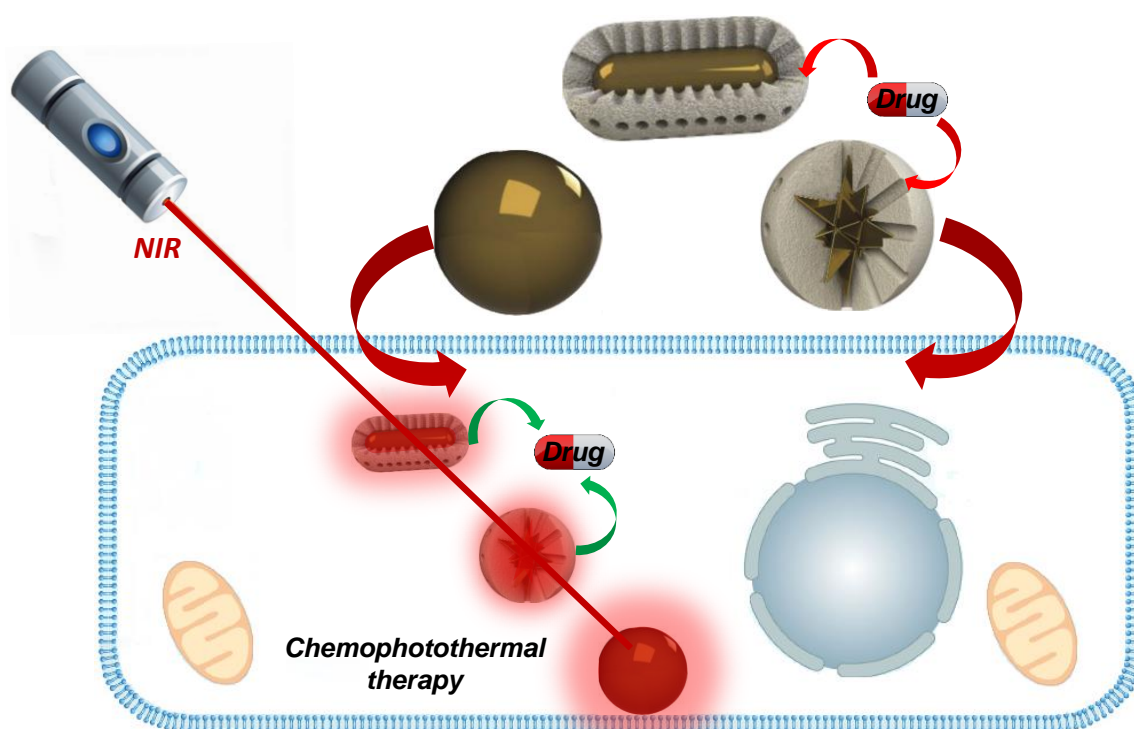


Figure 6. Au-Silica based composites for photothermal applications. Gold nanorods, nanostars and nanoshells are able to transform near infrared irradiation into thermal energy. The combination of such remote stimulus with drug delivery opens new possibilities for highly efficient therapeutic nanodevices. Unfortunately, the poor biodegradability of Au species makes their application poorly recommended for many treatments.

In addition to the strategy that employs Au embedded in a MS matrix, it is possible to carry out the opposite strategy, where Au particles are on the surface of regular MSNs. In addition to the expected greater sensitivity to stimulation with NIR, this strategy may simplify the gating process as the own AuNPs can act as nanogates [421–432]. This coating strategy was followed by Li *et al.* to develop thermoresponsive nanodevices with multimodal imaging possibilities using GNSts [422–433]; demonstrating their adequacy for multimodal, ultrasonic, tomographic, photoacoustic and photothermal induced imaging. However, despite the promising future for these Au species, their *in vivo* behavior should be extensively evaluated.

In a parallel way, there are another family of Au-Silica hybrids that present a similar distribution of components: Gold Nanoshells (GNSs)[423–434]. Those materials are prepared by coating a template with a thin Au layer, being silica an outstanding platform for it because of its NIR transparency. Like Nanostars, GNSs could be employed for generating PTE, but not for the controlled delivery of drugs as the template is sacrificed in a non-degradable coating. Like bare GNRs, nanoshells can be easily functionalized employing the known reactivity of Au; but contrary to smaller particles, GNSs must be carefully employed in intravenous formulations as their great size and highly difficult elimination will cause a severe accumulation and thus a long-lasting remainder effects. Nevertheless, those GNSs could be used on topic applications as elegantly demonstrated by Mitragotri [424–435] (Figure 7) and Nie [425–436], who employed those materials for treating acne and melanoma respectively. Moreover, a PEG-coated silica-gold nanoshells have entered clinical trials for thermal ablation of solid primary and/or metastatic lung tumors (ClinicalTrials.gov identifier: NCT01679470), giving more arguments for silica to be used on nanomedical devices.

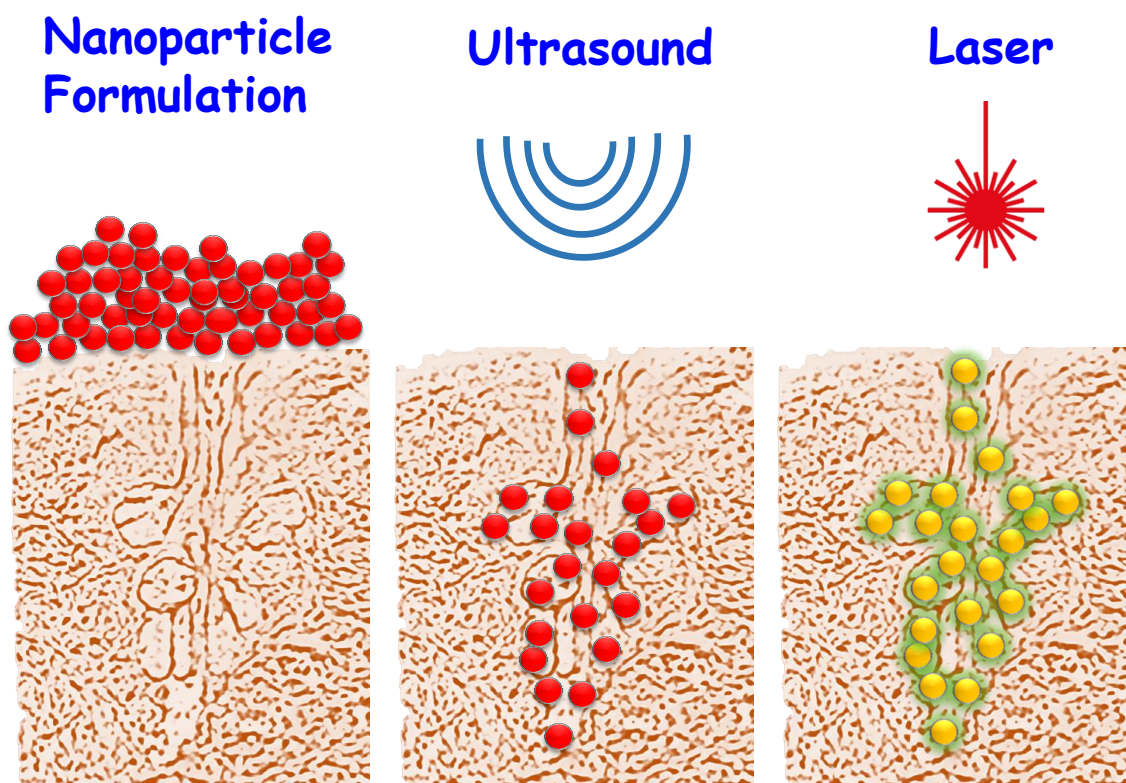


Figure 7. Two-step application of AuNSs for the treatment of acne. In this case the topical administration of the AuNSs, reduces significantly the risks associated to the “big” Au species.

In addition to Au species, there have been reported other degradable systems with plasmonic properties [426137]. Among them, CuS has arisen as the most recurrent component among inorganic materials [408,109119,120]. Like other PS, CuS has been successfully embedded into MS matrices to obtain functional photothermally active composites. On the first example reported Song *et al.* prepared Cu₉S₈@mSiO₂-PEG hybrids to treat Hep3B cells with simultaneous PTCT [427138], demonstrating a comparable loading capacity than the analogs containing GNRs. Additionally, hemolysis rates were similar for those obtained with PEG coated MS; thus validating the use of those nanocomposites suitable for combination therapy. Deepening on the topic, Zhu and coworkers employed an equivalent composite to successfully treat HeLa cells with a similar outcome [428139].

Besides PTE, CuS@MS composites have been also successfully employed in the development of materials for infrared thermal imaging and thermally responsive gated nanodevices. Along this line Zhang *et al.* reported the construction of a thermally triggered drug delivery nanodevices employing CuS@MS bearing aptamer-based nanogates [429140]. The resulting system was able to address MCF-7 cells due to the targeting capabilities of the aptamer and promote drug release when irradiated. For more information about the possibilities offered by DNA to develop mesopores' gates and targeting, please check reference [430141].

In addition to the use of MS as coating component, CuS nanoparticles could also act as gatekeepers [431142]. In this model the authors employed a S-S cleavable linker to connect MSNs and CuS nanoparticles, enabling GSH redox-mediated cleavage of the system in intracellular environments. The viability studies showed cooperative apoptotic effects when the release of DOX was combined with the oxidative stress generated by GSH depletion and the induction of PTE throughout NIR irradiation.

In another interesting approach, Huang and coworkers prepared CuS crystals within the MSNs' mesopores employing thermal decomposition of Cu thiolates [431143]. In a latter step the authors functionalized the outer MS layer with the Ir-2 PS, thus enabling dual photothermodynamic combination therapy. The system was activated when the typical radiations for each component (535

and 1064 nm) wavelengths were employed, permitting to destroy HeLa xenografts in mice in less than 7 days.

Other blooming field for CuS-containing composites is radiomedicine [132,133,144,145]. In a visionary example on the topic, Cai and coworkers employed CuS@MS to create a traceable multifunctional nanodevice with targeting abilities. To do so, they decorated the outer MS layer with a TRC105 human/murine chimeric IgG1 monoclonal antibody and a ⁶⁴Cu-chelated DOTA ligand [134,146]. The resulting system combined (1) a highly effective targeting with (2) enhanced detection provided by the radioisotope and (3) the possibility of exerting PTE. This model, evaluated in a murine model, demonstrated a complete tumor destruction when photoablation was exerted.

In addition to the photothermal effect described for Au and CuS species, very recently iron oxide nanoparticles have been reported to have a similar behavior [121,122,147]. This is of interest because the dual mode of action permits to access either deep tissues employing magnetic activation and surface tissues with light stimulation together with the MRI contrast capabilities of Fe oxides. Unfortunately, despite the enormous potential of combining magnetic and light excitation with a single device, up to our knowledge no studies on PTT in core-shell IOMSNs have been conducted yet.

In summary, in the light of the reported examples, it is clear that combined PTCT increases the effect of independent therapies. Nevertheless, those results must be accounted carefully as the PTE itself is able to completely destroy tissues if enough irradiation is applied. This effect, known as photoablation, is very useful to apply different degrees of tissue destruction depending on the disease. Although it may be useful for treating highly resistant or difficult-to-operate tumors, it will always occurs at the expense of destroying completely the tissues. However, despite the huge potential of these materials, up to date no Au-based nanoparticles are approved by the FDA, although barely modified Au nanorods and nanoshells claim to be in the pipeline [1,2,135,148,149,136]. Under these circumstances, it is logic to assume that biosafety and biocompatibility of Au-MS hybrids will take several years to become an available information. Indeed, to advance in the use Au for PTE, there is necessary to solve a number of unanswered questions like the power and duration of irradiation for an optimal therapeutic effect in different organs and tissues. But also there must be information about the adequate thickness [137,150] and morphology [138,151] of the mesoporous matrix and its possible thermal insulating effect; but also about the toxicity [139,152], degradation and excretion processes related to nanomaterials for PTE.

3.3. Nanocomposites for Photodynamic Therapy.

As outlined previously PDE is a therapeutic effect based on the generation of ROS. However, in order to fulfill their function, it is important that ROS can effectively diffuse into the cytosol before self-destruction; so therefore, their generation should occur at the outermost surface of the nanosystems. Hence, it is logic to assume that the classical core-shell architecture in which the PS occupies the central position is not the more convenient, as the ROS must get through the dense MS matrix. This circumstance made the researchers to be interested in in surface decorated systems, which are easy to prepare employing organic photosensitizers [97,108]. In addition to the previous, many researchers have also identified the generation of ROS as a side relaxation process after PTE generation. This could be employed to design multiple apoptotic inducing systems with a single photon excitation. Interesting examples have been described with Au [140,153], CuS and CoS [144,154], although none in combination with MS. For an outstanding and recent review on the modification of MSNs with different PS for PDE, please check references [142,155,156] (Figure 8).

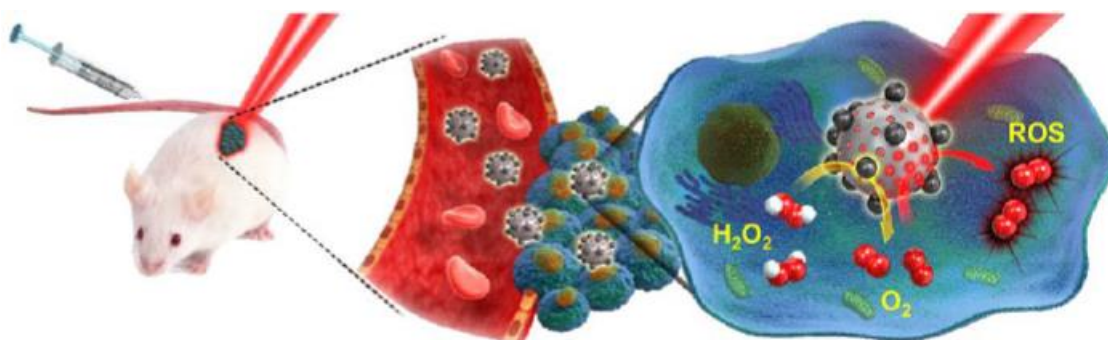


Figure 8. Photodynamic effect in therapy the light stimulation of is able to generate highly reactive oxygen species induce cellular apoptosis throughout oxidative stress and depletion of reductive species such as glutathione. The use of such dyes must be carefully addressed if they show long residence times, as their remainder activity may induce acute light sensitivity and chronic toxicity. Adapted from reference [143156].

3.4. Nanomaterials with light response: Fluorescence and Upconversion.

Fluorescence and Upconversion are two similar phenomena; both implicate the absorption of photons and their transformation into an emission of different wavelength. The difference between these two processes relies on the wavelength of the resulting emissions. So, while the fluorescence produces a lower energy radiation, the upconversion transforms low energy photons into a high energy radiation *via* a sequential excitation of the material throughout an anti-Stokes process. Obviously for accomplishing upconversion there are required to gather two or more photons.

As the outcome wavelength are different for both process, the application fields are different too. Fluorescence is the most important technique for detection of nanoparticles; being of interest for the detection and quantification of cell uptake and particles' trafficking, fate and excretion [144157]. While on the other hand, upconversion materials could be employed for either bright field detection (fluorescence) or photodynamic therapy if the resulting radiation is able to trigger an apoptotic process or to excite a PS [97108]. Herein, it is also important to remark that luminescence of UCNs is efficiently quenched by water, so the construction of composite materials must need from an intermediate dense silica layer to isolate the photoactive core.

Regarding the composition of these light-conversion materials, Upconversion Nanoparticles (UCNs) are generally formed by fluorides of lanthanide trivalent elements (La^{3+} , Gd^{3+} , Y^{3+} and Yb^{3+}) which have replaced some of the cations by dopant elements such as rare earth metals like Yb^{3+} , Er^{3+} , Tm^{3+} , etc. [145–147158–160]. On the other hand, excluding non-degradable C-dots [161–163148–150], Quantum Dots (QDs) are mainly composed by nanocrystalline metal chalcogenides (Zn^{2+} , Cd^{2+} or Pb^{2+} plus S^{2-} or Se^{2-}) among many other minor compositions [151,152164,165]. As could be figured out, the composition of these kind of materials may have a relevant impact on the biosafety of both UCNs [153166] and QDs [154,155167,168]; although this topic has been still very poorly covered. In any case it is logic to assume that their ionic nature, would favor an eventual full degradation throughout dissolution of crystals; which upon reaching a critical size, could be cleared out. However, their degradation occurs at the expense of releasing heavy metals [155–158168–171], selenides and fluorides [159172] into the organism. As a result, these nanocomposites must be very carefully applied as they are formed by poorly biocompatible and toxic elements which might expose the patient to a continuous dosage and undesired bioaccumulation. However, it is also important to note that the composite materials based on UCNs and QDs use very small crystals that could be quickly cleared upon degradation of the composites; although again, not much information is available on this topic.

The use of MS for the development of light-responsive composite nanomaterials allow to incorporate a porous layer which could be easily functionalized with polymers or targeting compounds and loaded with additional therapeutic compounds. Moreover, for most of applications

this MS matrix is highly transparent, which ensures a proper response of the light sensitive component [as long as the rest of components do not interfere with the incoming radiation](#).

3.5. Quantum Dot nanocomposites for bright field detection.

Fluorescence imaging is by far the most exploited tool for the detection, trafficking and bioaccumulation determination of nanoparticles in biomedical applications. Fluorophores could be either of organic nature such as fluorescein and its derivatives or inorganic, like quantum dots (QDs) and carbon dots [[148161](#)]. Along this line, organic fluorophores have been successfully employed to prepare Cornell dots, which are the first in-human clinical trial for a silica nanocomposite. Those silica nanoparticles, loaded with the Cy5 fluorophore are functionalized with a PEG coating, and a ^{124}I radiolabeled cRGDY targeting peptide (ClinicalTrials.gov identifier: NCT01266096), are able to accomplish integrin recognition and hence to detect melanoma and brain tumors [[160173](#)]. On the other side, QDs offer advantages over the organic molecules, as they do not suffer from quenching and show higher quantum efficiencies with narrow adsorption and emission bands. The biocompatibility and the biomedical uses of QDs are highly dependent on their composition, which besides containing heavy metals, also include poorly biocompatible solvents employed on their synthesis [[150,152,154,156,161163,165,167,169,174](#)]. This issue could be partially solved by coating QDs with a silica/MS layer able to displace the coordinated solvents while preserving [[162175](#)] the QD core [[163–165176–178](#)]. Unfortunately, the intrinsic toxicity associated to the forming elements and remainder solvents in their composition make them risky for *in vivo* biomedical applications. Nevertheless their outstanding luminescence make them ideal candidates for bioimaging and biosensors, as could be guessed by the overwhelming number of publications in these fields [[166–169179–182](#)].

3.6. Mesoporous Silica containing Upconversion Nanocomposites

Contrary to QDs, upconversion nanoparticles absorb low-energy photons and turn them into a higher energy emission. This property, interesting for the development of nanoprobe and sensors [[170183](#)], is also of interest for the development of therapeutic agents if the emission is energetic enough to perform cellular damage [[171,172184,185](#)]. For achieving so, light upconversion is usually combined with photosensitizers.

In the first example of this kind, Idris *et al.* built a nanocomposite in which an Yb/Er doped NaYF₄ UCN was coated with a MS layer containing two PDE sensitizers: Zinc phthalocyanine (ZnPC), merocyanine 540 (MC540) [[173186](#)]. This system was able to convert the incident 980 NIR radiation (2.5 W/cm², 40 min) into visible radiation (550 and 660 nm respectively) able to independently activate each photosensitizer. The system was evaluated against B16-F0 melanoma tumors in a murine model employing both naked or folate-PEG surface modifications. Under these circumstances the targeted systems achieved a higher tumor growth disruption although without tumor remission. More recently Wu, He and coworkers improved the targeting ability of this system employing a novel biomimetic camouflage strategy using stem-cell membranes [[174187](#)]. The resulting upconverting protocells showed good stability and biocompatibility together with a prolonged blood circulation time and the tumor-tropic properties of stem-cells. The triggering of the proapoptotic PDE with this nanodevice permitted to reduce significantly the progression of HeLa tumors in mice; but only when the UCN@MS were coated. This result showed the huge potential of membrane-coated nanosystems for cancer treatment. Additionally, this strategy could be also employed for enhancing long-time circulation and low immunogenic response, as elegantly reported by Xuan *et al.* [[17679](#)], who cloaked their nanoparticles with red-blood cell membranes with outstanding results.

The previous examples profited from a double sensitizer photodynamic therapy to develop highly efficient cancer therapies; however, in those examples mesopores were not occupied with any therapeutic agent. To cover this gap, Bu, Shi and coworkers developed a system for treating tumors with a synergistic reductive therapy based on the use of UCNs, together with a PS and a prodrug [[175188](#)]. For doing so the authors assumed that upon PDE triggering (ROS generation) hypoxic

environments are created. Therefore, if a prodrug that is activated under hypoxic conditions is co-administered, the apoptotic effect would be increased. The reported system employed Yb/Er/Gd doped NaYF₄ UCNs coated with silica as platform, silicon phthalocyanine dihydroxide as PS and tirapazamine as prodrug. The potential therapeutic effect of the whole system onto HeLa murine xenograft tumors provided promising tumor growth inhibition despite it was a non-targeted nanosystem, demonstrating again the potential of combination therapy (Figure 9).

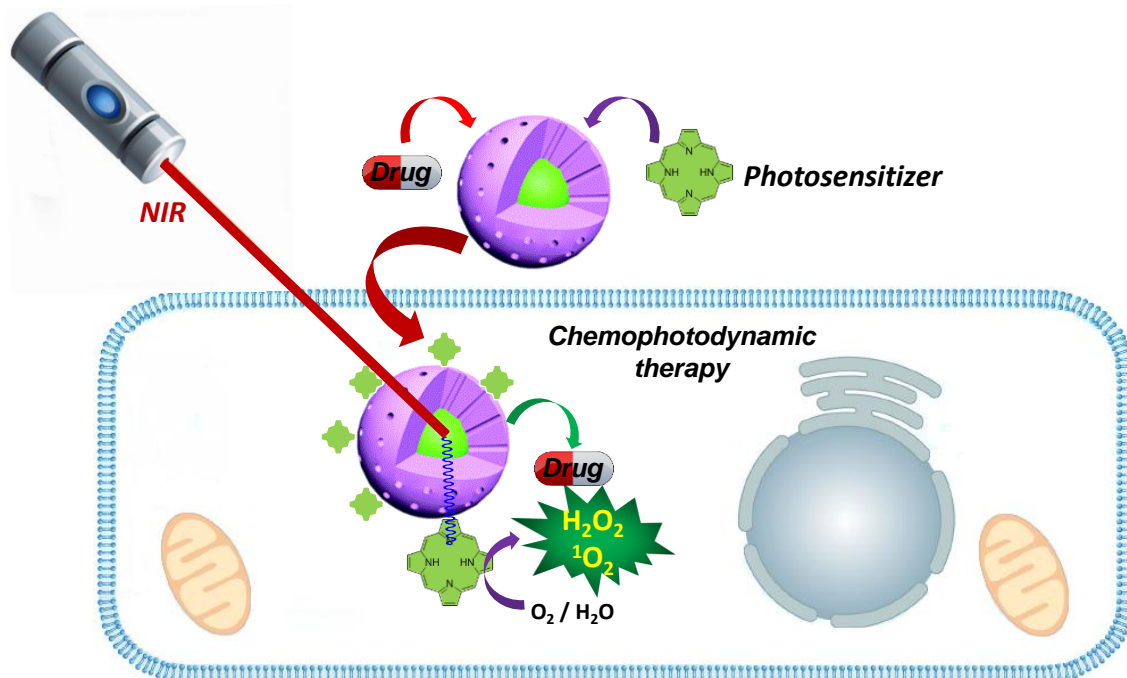


Figure 9. Upconversion-Silica based composites for photodynamic therapy. The internal core of those species is able to transform near infrared irradiation into high energetic UV-Vis radiation suitable for exciting most of photodynamic sensitizers, known to generate oxidative stress mediated apoptosis.

Additionally, UCNs@MS have been also successfully employed for drug delivery. In another contribution by Bu and Shi, an UV-Vis triggered azobenzene based nanoimpeller was employed to increase the outflow of DOX from the mesopores. In this case the system was completed with the fusogenic TAT peptide as targeting element [476189]. The authors claimed that the UCN was able to convert the incident NIR light (2.4 W/cm²) into a radiation able to photoisomerize the azobenzene and hence to favor the drug release acting as pore nanoimpellers. The *in vitro* evaluation on HeLa cells of the resulting system provided a nice correlation between irradiation time (5, 10, 15 and 20 minutes) and cell mortality. The authors associated the higher death rates to higher DOX releases. However, Dong and Zink addressed an in-depth study of the nanoimpeller-mediated release mechanism [477190] finding that such enhanced DOX release did not occur due to photoisomerization. According to their investigations, the driving mechanism was a thermal effect created upon heating the UCN cores with the incoming 980 nm light; pointing out a PTE able to increase drug outflow, as demonstrated in light-induced drug release with UCN@MS in the absence of such nanoimpellers.

Other possible strategy to achieve PDE with UCN@MS composites is trapping the PS into the mesopores as demonstrated by Han *et al* [478191]. In their system the mesopores were loaded with Rose Bengal and capped with an adamantane–cyclodextrin nanogate. This approach although did not significantly improve the therapeutic potential of other reported systems, opened the door to massive delivery of PS, which could be of interest for defining tumor burdens in post-treatment surgeries.

Apart from upconversion of NIR into UV/Vis radiation, an interesting example has been reported for the downconversion process; although in this case the use of highly ionizing radiation

limits significantly the applicability. For so, Hirata's group designed a Gd-Al garnet for X-Rays downconversion [479192]. The system was completed with the Rose Bengal photodynamic sensitizer able to transform the downconverted light into ROS. Regarding this nanosystem, it is noteworthy that the Gd-Al garnet enabled two unprecedented features for light-activated nanomaterials: (1) enabled MRI detection and (2) the downconversion of X-rays permitted an unprecedented in-depth tissue remote activation of nanosystems.

4. Multicomponent nanocomposites containing mesoporous silica.

As already mentioned, the advantages of silica in the construction of nanomedical devices goes beyond its mere use as porous matrices. As reviewed, it also allows the connection of functional entities easily and quickly. In the case at hand, the construction of multifunctional systems, there are many examples that use silica to integrate different types of particles and create nanosystems responsive to more than one remote stimuli. Among all published combinations, the most common is one that uses light and magnetic stimulation simultaneously. Among them, the most common combination is the one that combines magnetic and light stimuli. To this end, many research groups employed already developed core-shell systems for the preparation of complex composites. Following this strategy, Gao *et al.* reported the development of a multilayered, folate targeted, Fe₃O₄@MS@CuS nanocomposite –able to accomplish targeted PTCT and MRI [480193]; while Yao *et al.* reported the preparation of Fe₃O₄@MS@QDs device able to perform drug delivery and magneto-photothermal therapy with an outstanding detectability [481194].

Besides the combination of SPIONs and AuNPs for magneto/photothermal therapy, this combination is also very useful for the preparation of multimodal detection systems, as the SPION enables MRI detection and Au does the same for X-rays computed tomography [482195]. With this purpose Yang *et al.* prepared a multimodal detectable nanosystem in which a Fe₃O₄@Au composite was embedded into a MS matrix [483196]. This system was further modified with three apoptotic inducers: a PS for PDE, DOX and a siRNA, which permitted to obtain a tumor growth reversal in a MCF-7/ADR cells. Another multipurpose assembly of AuNPs and SPIONs, reported by Sánchez *et al.*, grew AuNPs onto IOMSNs. The resulting anisotropic Au-coated *Janus*-Fe₃O₄@MS composites [484197] were able to perform MRI and computed tomography imaging. But in addition to previous systems, the incorporation of a fluorescent Alexa Fluor 647 dye onto the exposed part of AuNPs, permitted to enable conventional bright field optical detection too. Apart from Au, IOMSNs have been also combined with different inorganic species. For example, Cui and coworkers employed a silica coated Fe₃O₄@ZnO composite to achieve microwave-triggered drug release. In this case, the ZnO interlayer can acted as ultrasound-to-temperature converter although with poor efficiency [485198].

In the same way, core-shell UCN@MS composites have been also subject of additional modifications seeking for more versatile nanodevices for theranosis. Two examples with UCN cores were reported by (1) Shi and coworkers, who designed a system that combined radio- and photothermal ablation by using ultrafine radioactive CuS nanoparticles deposited onto a UCN@SiO₂ platform [486199]; and (2) by Liu *et al.* who successfully coated UCN@MS with SPIONs for accomplishing bioimaging plus magnetically targeted DOX delivery [487200]. Both examples, permitted to obtain great tumor destruction rates on murine models, demonstrating once again the potential of combining different functionalities into a nanodevice.

As reviewed so far, the combination of functional components in single nanometric formulations permits to combine apoptotic effects and hence to achieve better therapeutic profiles in the treatment of cancer. Unfortunately, to use these systems, there must be considered a large number of biosafety limitations. Those are not only consequence of the increasing complexity and number of connecting components, but also may be consequences of unforeseen side-effects that may arise when– different functional components coexist in complex, living systems.

5. Conclusions.

~~Although raw silica nanoparticles are not approved nor employed as a pharmaceutical formulations, the use of mesoporous silica is widespread in the preparation of functional nanodevices~~ Despite raw mesoporous silica nanoparticles have been not approved as a nanomedical formulations, the use of silica is widespread in the preparation of functional nanodevices. This is due to its extraordinary physicochemical behavior, biocompatibility, degradability and porous morphology. For this reason, materials formulated with silica in their composition have entered for the first time in the clinical studies pipeline; although there is still a long way to go before its use generalizes.

From the data presented herein, there could be concluded that silica is no longer a material to be discarded by the pharmaceutical companies. Indeed, it must be considered and properly studied as one more possible component for nanoformulations, since it provides a unique plasticity to manufacture multifunctional devices. Above all, this must be tackled with rigorous studies of acute and long-term toxicity, bioaccumulation and clearance of nanosized silica to set a basis for modelling future composites. ~~From a technical point of view, it is important to note that silica is a material that presents high permeation to (electro)magnetic fields and transparency against ultraviolet and infrared radiation, which allow to maintain unaltered the properties of the functional components~~ From a technical point of view, it is important to note that silica is a material that presents high permeation to (electro)magnetic fields and transparency against ultraviolet and infrared radiations, which is of interest for obtaining adequate remote activation of functional components. In short, in light of the published results, our opinion is that the use of silica in composite materials favors its translation into clinical phases, since unlike other components, the use of silica does not require a large number of connectors, complex synthesis processes or poorly stable components.

Acknowledgements: The authors want to acknowledge financial support from European Research Council ERC-2015-AdG-694160] and Ministerio de Economía y Competitividad MAT2015-64831-RJ. R.R.C specially acknowledges Centro de Investigación Biomédica en Red for a postdoctoral contract.

Abbreviations

Doxorubicin (DOX); Food and Drug Administration (FDA); Glutathione (GSH); Gold Nanoparticles (AuNPs); Gold Nanorods (GNRs); Gold Nanoshells (GNSs); Gold Nanostars (GNSts); Iron Oxide-Mesoporous Silica Nanocomposites (IOMSNs); Magnetic Drug Delivery Systems (MDDS); Magnetic Resonance Imaging (MRI); Magnetothermal-Chemotherapy (MTCT); Mesoporous Silica (MS); Mesoporous Silica Coated Gold Nanorods (MSGNRs); Mesoporous Silica-Metal Oxide Nanocomposites (MSMONs); Mesoporous Silica Nanoparticles (MSNs); Micro RiboNucleic Acid (miRNA); Near Infrared Radiation (NIR); Photodynamic Effect (PDE); Photosensitizer (PS); Photothermal Effect (PTE); Photothermal-Chemotherapy (PTCT); Quantum Dots (QDs); Reactive Oxygen Species (ROS); Small Interfering RiboNucleic Acid (siRNA); Superparamagnetic Iron Oxide Nanoparticles (SPIONs); Upconversion Nanoparticles (UCNs)

Reference

1. Anselmo, A. C.; Mitragotri, S. Nanoparticles in the clinic. *Bioeng. Transl. Med.* **2016**, *1*, 10–29. doi:10.1002/btm2.10003.
2. Anselmo, A. C.; Mitragotri, S. A Review of Clinical Translation of Inorganic Nanoparticles. *AAPS J.* **2015**, *17*, 1041–1054. doi:10.1208/s12248-015-9780-2.
3. Hao, R.; Xing, R.; Xu, Z.; Hou, Y.; Gao, S.; Sun, S. Synthesis, Functionalization, and Biomedical Applications of Multifunctional Magnetic Nanoparticles. *Adv. Mater.* **2010**, *22*, 2729–2742. doi:10.1002/adma.201000260.
4. Wu, L.; Mendoza-Garcia, A.; Li, Q.; Sun, S. Organic Phase Syntheses of Magnetic Nanoparticles and Their Applications. *Chem. Rev.* **2016**, *116*, 10473–10512. doi:10.1021/acs.chemrev.5b00687.
5. Huang, X.; Jain, P. K.; El-Sayed, I. H.; El-Sayed, M. A. Plasmonic photothermal therapy (PPTT) using gold nanoparticles. *Lasers Med. Sci.* **2008**, *23*, 217–228.

- doi:10.1007/s10103-007-0470-x.
6. Huang, X.; Jain, P. K.; El-Sayed, I. H.; El-Sayed, M. A. Gold nanoparticles: interesting optical properties and recent applications in cancer diagnostics and therapy. *Nanomedicine* **2007**, *2*, 681–693. doi:10.2217/17435889.2.5.681.
 7. Liu, B.; Li, C.; Cheng, Z.; Hou, Z.; Huang, S.; Lin, J. Functional nanomaterials for near-infrared-triggered cancer therapy. *Biomater. Sci.* **2016**, *4*, 890–909. doi:10.1039/c6bm00076b.
 8. Sercombe, L.; Veerati, T.; Moheimani, F.; Wu, S. Y.; Sood, A. K.; Hua, S. Advances and Challenges of Liposome Assisted Drug Delivery. *Front. Pharmacol.* **2015**, *6*, 286. doi:10.3389/fphar.2015.00286.
 9. Allen, T. M.; Cullis, P. R. Liposomal drug delivery systems: From concept to clinical applications. *Adv. Drug Deliv. Rev.* **2013**, *65*, 36–48. doi:10.1016/j.addr.2012.09.037.
 10. Vallet-Regí, M.; Rámila, A.; del Real, R. P.; Pérez-Pariente, J. A New Property of MCM-41: Drug Delivery System. *Chem. Mater.* **2001**, *13*, 308–311. doi:10.1021/cm0011559.
 11. Vallet-Regí, M.; Balas, F.; Arcos, D. Mesoporous Materials for Drug Delivery. *Angew. Chemie Int. Ed.* **2007**, *46*, 7548–7558. doi:10.1002/anie.200604488.
 12. Singh, P.; Sen, K. Contemporary mesoporous materials for drug delivery applications: a review. *J. Porous Mater.* **2018**, *25*, 965–987. doi:10.1007/s10934-017-0508-9.
 13. Soenen, S. J.; Velde, G. Vande; Ketkar-Atre, A.; Himmelreich, U.; De Cuyper, M. Magnetoliposomes as magnetic resonance imaging contrast agents. *Wiley Interdiscip. Rev. Nanomedicine Nanobiotechnology* **2011**, *3*, 197–211. doi:10.1002/wnan.122.
 14. Monnier, C. A.; Burnand, D.; Rothen-Rutishauser, B.; Lattuada, M.; Petri-Fink, A. Magnetoliposomes: opportunities and challenges. *Eur. J. Nanomedicine* **2014**, *6*, 201–215. doi:10.1515/ejnm-2014-0042.
 15. Chauhan, D. S.; Prasad, R.; Devrukhkar, J.; Selvaraj, K.; Srivastava, R. Disintegrable NIR Light Triggered Gold Nanorods Supported Liposomal Nanohybrids for Cancer Theranostics. *Bioconjug. Chem.* **2018**, *29*, 1510–1518. doi:10.1021/acs.bioconjchem.7b00801.
 16. Hameed, S.; Bhattarai, P.; Dai, Z. Cerasomes and Bicelles: Hybrid Bilayered Nanostructures With Silica-Like Surface in Cancer Theranostics. *Front. Chem.* **2018**, *6*, 127. doi:10.3389/fchem.2018.00127.
 17. Buzea, C.; Pacheco, I. I.; Robbie, K. Nanomaterials and nanoparticles: Sources and toxicity. *Biointerphases* **2007**, *2*, MR17-MR71. doi:10.1116/1.2815690.
 18. Tang, F.; Li, L.; Chen, D. Mesoporous Silica Nanoparticles: Synthesis, Biocompatibility and Drug Delivery. *Adv. Mater.* **2012**, *24*, 1504–1534. doi:10.1002/adma.201104763.
 19. Croissant, J. G.; Fatieiev, Y.; Almalik, A.; Khashab, N. M. Mesoporous Silica and Organosilica Nanoparticles: Physical Chemistry, Biosafety, Delivery Strategies, and Biomedical Applications. *Adv. Healthc. Mater.* **2018**, *7*, 1700831. doi:10.1002/adhm.201700831.
 20. Li, Z.; Barnes, J. C.; Bosoy, A.; Stoddart, J. F.; Zink, J. I. Mesoporous silica nanoparticles in biomedical applications. *Chem. Soc. Rev.* **2012**, *41*, 2590–2605. doi:10.1039/c1cs15246g.
 21. Izquierdo-Barba, I.; Colilla, M.; Manzano, M.; Vallet-Regí, M. *In vitro* stability of SBA-15 under physiological conditions. *Microporous Mesoporous Mater.* **2010**, *132*, 442–452. doi:10.1016/j.micromeso.2010.03.025.
 22. Paris, J. L.; Colilla, M.; Izquierdo-Barba, I.; Manzano, M.; Vallet-Regí, M. Tuning mesoporous silica dissolution in physiological environments: a review. *J. Mater. Sci.* **2017**, *52*, 8761–8771. doi:10.1007/s10853-017-0787-1.
 23. Croissant, J. G.; Brinker, C. J. Biodegradable Silica-Based Nanoparticles: Dissolution Kinetics and Selective Bond Cleavage. In *The Enzymes*, vol. 43; Elsevier, 2018; pp. 181–214.
 24. Lindén, M. Biodistribution and Excretion of Intravenously Injected Mesoporous Silica Nanoparticles: Implications for Drug Delivery Efficiency and Safety. In *The Enzymes*, vol. 43; Elsevier, 2018; pp. 155–180.
 25. Shang, L.; Nienhaus, K.; Nienhaus, G. Engineered nanoparticles interacting with cells: size matters. *J. Nanobiotechnology* **2014**, *12*, 5. doi:10.1186/1477-3155-12-5.

26. Huang, X.; Teng, X.; Chen, D.; Tang, F.; He, J. The effect of the shape of mesoporous silica nanoparticles on cellular uptake and cell function. *Biomaterials* **2010**, *31*, 438–448. doi:10.1016/j.biomaterials.2009.09.060.
27. Huang, X.; Li, L.; Liu, T.; Hao, N.; Liu, H.; Chen, D.; Tang, F. The Shape Effect of Mesoporous Silica Nanoparticles on Biodistribution, Clearance, and Biocompatibility *in vivo*. *ACS Nano* **2011**, *5*, 5390–5399. doi:10.1021/nn200365a.
28. Li, L.; Liu, T.; Fu, C.; Tan, L.; Meng, X.; Liu, H. Biodistribution, excretion, and toxicity of mesoporous silica nanoparticles after oral administration depend on their shape. *Nanomedicine Nanotechnology, Biol. Med.* **2015**, *11*, 1915–1924. doi:10.1016/j.nano.2015.07.004.
29. Li, J.; Shen, S.; Kong, F.; Jiang, T.; Tang, C.; Yin, C. Effects of pore size on *in vitro* and *in vivo* anticancer efficacies of mesoporous silica nanoparticles. *RSC Adv.* **2018**, *8*, 24633–24640. doi:10.1039/C8RA03914C.
30. Napierska, D.; Thomassen, L. C. J.; Rabolli, V.; Lison, D.; Gonzalez, L.; Kirsch-Volders, M.; Martens, J. A.; Hoet, P. H. Size-Dependent Cytotoxicity of Monodisperse Silica Nanoparticles in Human Endothelial Cells. *Small* **2009**, *5*, 846–853. doi:10.1002/sml.200800461.
31. Nishimori, H.; Kondoh, M.; Isoda, K.; Tsunoda, S.; Tsutsumi, Y.; Yagi, K. Silica nanoparticles as hepatotoxicants. *Eur. J. Pharm. Biopharm.* **2009**, *72*, 496–501. doi:10.1016/j.ejpb.2009.02.005.
32. McCarthy, J.; Inkiewicz-Stepniak, I.; Corbalan, J. J.; Radomski, M. W. Mechanisms of Toxicity of Amorphous Silica Nanoparticles on Human Lung Submucosal Cells *in vitro*: Protective Effects of Fisetin. *Chem. Res. Toxicol.* **2012**, *25*, 2227–2235. doi:10.1021/tx3002884.
33. Meng, H.; Yang, S.; Li, Z.; Xia, T.; Chen, J.; Ji, Z.; Zhang, H.; Wang, X.; Lin, S.; Huang, C.; Zhou, Z. H.; Zink, J. I.; Nel, A. E. Aspect Ratio Determines the Quantity of Mesoporous Silica Nanoparticle Uptake by a Small GTPase-Dependent Macropinocytosis Mechanism. *ACS Nano* **2011**, *5*, 4434–4447. doi:10.1021/nn103344k.
34. Croissant, J. G.; Fatieiev, Y.; Khashab, N. M. Degradability and Clearance of Silicon, Organosilica, Silsesquioxane, Silica Mixed Oxide, and Mesoporous Silica Nanoparticles. *Adv. Mater.* **2017**, *29*, 1604634. doi:10.1002/adma.201604634.
35. Ramzy, L.; Nasr, M.; Metwally, A. A.; Awad, G. A. S. Cancer nanotheranostics: A review of the role of conjugated ligands for overexpressed receptors. *Eur. J. Pharm. Sci.* **2017**, *104*, 273–292. doi:10.1016/j.ejps.2017.04.005.
36. Baeza, A.; Colilla, M.; Vallet-Regí, M. Advances in mesoporous silica nanoparticles for targeted stimuli-responsive drug delivery. *Expert Opin. Drug Deliv.* **2015**, *12*, 319–337. doi:10.1517/17425247.2014.953051.
37. Baeza, A.; Vallet-Regí, M. Targeted Mesoporous Silica Nanocarriers in Oncology. *Curr. Drug Targets* **2018**, *19*, 213–224. doi:10.2174/1389450117666160603023037.
38. Pisani, C.; Gaillard, J. C.; Dorandeu, C.; Charnay, C.; Guari, Y.; Chopineau, J.; Devoisselle, J. M.; Armengaud, J.; Prat, O. Experimental separation steps influence the protein content of corona around mesoporous silica nanoparticles. *Nanoscale* **2017**, *9*, 5769–5772. doi:10.1039/C7NR01654A.
39. Pisani, C.; Gaillard, J.-C.; Odorico, M.; Nyalosaso, J. L.; Charnay, C.; Guari, Y.; Chopineau, J.; Devoisselle, J.-M.; Armengaud, J.; Prat, O. The timeline of corona formation around silica nanocarriers highlights the role of the protein interactome. *Nanoscale* **2017**, *9*, 1840–1851. doi:10.1039/C6NR04765C.
40. He, Q.; Zhang, J.; Shi, J.; Zhu, Z.; Zhang, L.; Bu, W.; Guo, L.; Chen, Y. The effect of PEGylation of mesoporous silica nanoparticles on nonspecific binding of serum proteins and cellular responses. *Biomaterials* **2010**, *31*, 1085–1092. doi:10.1016/j.biomaterials.2009.10.046.
41. Cauda, V.; Argyo, C.; Bein, T. Impact of different PEGylation patterns on the long-term bio-stability of colloidal mesoporous silica nanoparticles. *J. Mater. Chem.* **2010**, *20*, 8693–8699. doi:10.1039/c0jm01390k.
42. Estephan, Z. G.; Jaber, J. A.; Schlenoff, J. B. Zwitterion-Stabilized Silica Nanoparticles: Toward Nonstick Nano. *Langmuir* **2010**, *26*, 16884–16889. doi:10.1021/la103095d.
43. Khung, Y. L.; Narducci, D. Surface modification strategies on mesoporous silica

- nanoparticles for anti-biofouling zwitterionic film grafting. *Adv. Colloid Interface Sci.* **2015**, *226*, 166–186. doi:10.1016/j.cis.2015.10.009.
44. [Gulin-Sarfraz, T.; Zhang, J.; Desai, D.; Teuho, J.; Sarfraz, J.; Jiang, H.; Zhang, C.; Sahlgren, C.; Lindén, M.; Gu, H.; Rosenholm, J. Combination of magnetic field and surface functionalization for reaching synergistic effects in cellular labeling by magnetic core-shell nanospheres. *Biomater. Sci.* **2014**, *2*, 1750–1760. doi: 10.1039/C4BM00221K.](#)
45. [Sun, Z.; Zhou, X.; Luo, W.; Yue, Q.; Zhang, Y.; Cheng, X.; Li, W.; Kong, B.; Deng, Y.; Zhao, D. Interfacial engineering of magnetic particles with porous shells: Towards magnetic core – Porous shell microparticles. *Nano Today* **2016**, *11*, 464–482, doi:10.1016/j.nantod.2016.07.003](#)
46. [Karaman, D. S.; Sarparanta, M. P.; Rosenholm, J. M.; Airaksinen, A. J. Multimodality Imaging of Silica and Silicon Materials In Vivo. *Adv. Mater.* **2018**, *30*, 1703651, doi:10.1002/adma.201703651](#)
4447. Giner-Casares, J. J.; Henriksen-Lacey, M.; Coronado-Puchau, M.; Liz-Marzán, L. M. Inorganic nanoparticles for biomedicine: where materials scientists meet medical research. *Mater. Today* **2016**, *19*, 19–28. doi:10.1016/j.mattod.2015.07.004.
4548. Lu, A.-H.; Salabas, E. L.; Schüth, F. Magnetic Nanoparticles: Synthesis, Protection, Functionalization, and Application. *Angew. Chemie Int. Ed.* **2007**, *46*, 1222–1244. doi:10.1002/anie.200602866.
4649. Laurent, S.; Forge, D.; Port, M.; Roch, A.; Robic, C.; Vander Elst, L.; Muller, R. N. Magnetic Iron Oxide Nanoparticles: Synthesis, Stabilization, Vectorization, Physicochemical Characterizations, and Biological Applications. *Chem. Rev.* **2008**, *108*, 2064–2110. doi:10.1021/cr068445e.
4750. Hedayatnasab, Z.; Abnisa, F.; Daud, W. M. A. W. Review on magnetic nanoparticles for magnetic nanofluid hyperthermia application. *Mater. Des.* **2017**, *123*, 174–196. doi:10.1016/j.matdes.2017.03.036.
4851. Na, H. Bin; Song, I. C.; Hyeon, T. Inorganic Nanoparticles for MRI Contrast Agents. *Adv. Mater.* **2009**, *21*, 2133–2148. doi:10.1002/adma.200802366.
4952. Busquets, M. A.; Estelrich, J.; Sánchez-Martín, M. J. Nanoparticles in magnetic resonance imaging: from simple to dual contrast agents. *Int. J. Nanomedicine* **2015**, *10*, 1727–1741. doi:10.2147/IJN.S76501.
5053. Šafařík, I.; Šafaříková, M. Magnetic Nanoparticles and Biosciences. In *Nanostructured Materials*; Springer Vienna: Vienna, 2002; pp. 1–23.
5154. Chowdhury, M. A. Design, Development and Applications of the Silica-Based Contrast Agents in Magnetic Resonance Imaging. *Curr. Nanomedicine* **2018**, *8*, 3–27. doi:10.2174/2468187307666171019162332.
5255. Castillo, R. R.; Colilla, M.; Vallet-Regí, M. Advances in mesoporous silica-based nanocarriers for co-delivery and combination therapy against cancer. *Expert Opin. Drug Deliv.* **2017**, *14*, 229–243. doi:10.1080/17425247.2016.1211637.
5356. Nasrallah, G. K.; Zhang, Y.; Zagho, M. M.; Ismail, H. M.; Al-Khalaf, A. A.; Prieto, R. M.; Albinali, K. E.; Elzatahry, A. A.; Deng, Y. A systematic investigation of the bio-toxicity of core-shell magnetic mesoporous silica microspheres using zebrafish model. *Microporous Mesoporous Mater.* **2018**, *265*, 195–201. doi:10.1016/j.micromeso.2018.02.008.
5457. He, Q.; Zhang, J.; Shi, J.; Zhu, Z.; Zhang, L.; Bu, W.; Guo, L.; Chen, Y. The effect of PEGylation of mesoporous silica nanoparticles on nonspecific binding of serum proteins and cellular responses. *Biomaterials* **2010**, *31*, 1085–1092. doi:10.1016/j.biomaterials.2009.10.046.
5558. He, Q.; Zhang, Z.; Gao, F.; Li, Y.; Shi, J. In vivo Biodistribution and Urinary Excretion of Mesoporous Silica Nanoparticles: Effects of Particle Size and PEGylation. *Small* **2011**, *7*, 271–280. doi:10.1002/smll.201001459.
5659. Rascol, E.; Daurat, M.; Da Silva, A.; Maynadier, M.; Dorandeu, C.; Charnay, C.; Garcia, M.; Lai-Kee-Him, J.; Bron, P.; Auffan, M.; Liu, W.; Angeletti, B.; Devoisselle, J.-M.; Guari, Y.

- Gary-Bobo, M.; Chopineau, J. Biological Fate of Fe₃O₄ Core-Shell Mesoporous Silica Nanoparticles Depending on Particle Surface Chemistry. *Nanomaterials* **2017**, *7*, 162. doi:10.3390/nano7070162.
- [5760](#). Cheng, W.; Nie, J.; Xu, L.; Liang, C.; Peng, Y.; Liu, G.; Wang, T.; Mei, L.; Huang, L.; Zeng, X. pH-Sensitive Delivery Vehicle Based on Folic Acid-Conjugated Polydopamine-Modified Mesoporous Silica Nanoparticles for Targeted Cancer Therapy. *ACS Appl. Mater. Interfaces* **2017**, *9*, 18462–18473. doi:10.1021/acsami.7b02457.
- [5861](#). Tian, Z.; Yu, X.; Ruan, Z.; Zhu, M.; Zhu, Y.; Hanagata, N. Magnetic mesoporous silica nanoparticles coated with thermo-responsive copolymer for potential chemo- and magnetic hyperthermia therapy. *Microporous Mesoporous Mater.* **2018**, *256*, 1–9. doi:10.1016/j.micromeso.2017.07.053.
- [5962](#). Guisasaola, E.; Asín, L.; Beola, L.; de la Fuente, J. M.; Baeza, A.; Vallet-Regí, M. Beyond Traditional Hyperthermia: *In vivo* Cancer Treatment with Magnetic-Responsive Mesoporous Silica Nanocarriers. *ACS Appl. Mater. Interfaces* **2018**, *10*, 12518–12525. doi:10.1021/acsami.8b02398.
- [6063](#). Yin, P. T.; Pongkulapa, T.; Cho, H.-Y.; Han, J.; Pasquale, N. J.; Rabie, H.; Kim, J.-H.; Choi, J.-W.; Lee, K.-B. Overcoming Chemoresistance in Cancer via Combined MicroRNA Therapeutics with Anticancer Drugs Using Multifunctional Magnetic Core-Shell Nanoparticles. *ACS Appl. Mater. Interfaces* **2018**, *10*, 26954–26963. doi:10.1021/acsami.8b09086.
- [6164](#). Xia, T.; Kovochich, M.; Liong, M.; Meng, H.; Kabehie, S.; George, S.; Zink, J. I.; Nel, A. E. Polyethyleneimine Coating Enhances the Cellular Uptake of Mesoporous Silica Nanoparticles and Allows Safe Delivery of siRNA and DNA Constructs. *ACS Nano* **2009**, *3*, 3273–3286. doi:10.1021/nn900918w.
- [6265](#). Cooperstein, M. A.; Canavan, H. E. Assessment of cytotoxicity of (N-isopropylacrylamide) and Poly(N-isopropylacrylamide)-coated surfaces. *Biointerphases* **2013**, *8*, 19. doi:10.1186/1559-4106-8-19.
- [6366](#). Yang, Q.; Lai, S. K. Anti-PEG immunity: emergence, characteristics, and unaddressed questions. *Wiley Interdiscip. Rev. Nanomedicine Nanobiotechnology* **2015**, *7*, 655–677. doi:10.1002/wnan.1339.
- [6467](#). Zhang, P.; Sun, F.; Liu, S.; Jiang, S. Anti-PEG antibodies in the clinic: Current issues and beyond PEGylation. *J. Control. Release* **2016**, *244*, 184–193. doi:10.1016/j.jconrel.2016.06.040.
- [6568](#). Popova, M.; Trendafilova, I.; Szegedi, Á.; Momekova, D.; Mihály, J.; Momekov, G.; Kiss, L. F.; Lázár, K.; Koseva, N. Novel SO₃H functionalized magnetic nanoporous silica/polymer nanocomposite as a carrier in a dual-drug delivery system for anticancer therapy. *Microporous Mesoporous Mater.* **2018**, *263*, 96–105. doi:10.1016/j.micromeso.2017.12.005.
- [6669](#). Sinha, A.; Chakraborty, A.; Jana, N. R. Dextran-Gated, Multifunctional Mesoporous Nanoparticle for Glucose-Responsive and Targeted Drug Delivery. *ACS Appl. Mater. Interfaces* **2014**, *6*, 22183–22191. doi:10.1021/am505848p.
- [6770](#). An, J.; Zhang, X.; Guo, Q.; Zhao, Y.; Wu, Z.; Li, C. Glycopolymer modified magnetic mesoporous silica nanoparticles for MR imaging and targeted drug delivery. *Colloids Surfaces A Physicochem. Eng. Asp.* **2015**, *482*, 98–108. doi:10.1016/j.colsurfa.2015.04.035.
- [6871](#). Gao, Q.; Xie, W.; Wang, Y.; Wang, D.; Guo, Z.; Gao, F.; Zhao, L.; Cai, Q. A theranostic nanocomposite system based on radial mesoporous silica hybridized with Fe₃O₄ nanoparticles for targeted magnetic field responsive chemotherapy of breast cancer. *RSC Adv.* **2018**, *8*, 4321–4328. doi:10.1039/C7RA12446E.
- [6972](#). Heggannavar, G. B.; Hiremath, C. G.; Achari, D. D.; Pangarkar, V. G.; Kariduraganavar, M. Y. Development of Doxorubicin-Loaded Magnetic Silica-Pluronic F-127 Nanocarriers Conjugated with Transferrin for Treating Glioblastoma across the Blood-Brain Barrier Using an *in vitro* Model. *ACS Omega* **2018**, *3*, 8017–8026. doi:10.1021/acsomega.8b00152.
- [7073](#). Portilho, F. L.; Helal-Neto, E.; Cabezas, S. S.; Pinto, S. R.; dos Santos, S. N.; Pozzo, L.; Sancenón, F.; Martínez-Mañez, R.; Santos-Oliveira, R. Magnetic core mesoporous silica nanoparticles doped with dacarbazine and labelled with ^{99m}Tc for early and differential

- detection of metastatic melanoma by single photon emission computed tomography. *Artif. Cells, Nanomedicine, Biotechnol.* **2018**, *46*, 1080–1087. doi:10.1080/21691401.2018.1443941.
- [7474](#). García, K. P.; Zarschler, K.; Barbaro, L.; Barreto, J. A.; O'Malley, W.; Spiccia, L.; Stephan, H.; Graham, B. Zwitterionic-Coated “Stealth” Nanoparticles for Biomedical Applications: Recent Advances in Countering Biomolecular Corona Formation and Uptake by the Mononuclear Phagocyte System. *Small* **2014**, *10*, 2516–2529. doi:10.1002/smll.201303540.
- [7275](#). Sanchez-Salcedo, S.; Vallet-Regí, M.; Shahin, S. A.; Glackin, C. A.; Zink, J. I. Mesoporous core-shell silica nanoparticles with anti-fouling properties for ovarian cancer therapy. *Chem. Eng. J.* **2018**, *340*, 114–124. doi:10.1016/j.cej.2017.12.116.
- [7376](#). Butler, K. S.; Durfee, P. N.; Theron, C.; Ashley, C. E.; Carnes, E. C.; Brinker, C. J. Protocells: Modular Mesoporous Silica Nanoparticle-Supported Lipid Bilayers for Drug Delivery. *Small* **2016**, *12*, 2173–2185. doi:10.1002/smll.201502119.
- [7477](#). Mattingly, S. J.; Otoole, M. G.; James, K. T.; Clark, G. J.; Nantz, M. H. Magnetic nanoparticle-supported lipid bilayers for drug delivery. *Langmuir* **2015**, *31*, 3326–3332. doi:10.1021/la504830z.
- [7578](#). Sharifabad, M. E.; Mercer, T.; Sen, T. Drug-loaded liposome-capped mesoporous core-shell magnetic nanoparticles for cellular toxicity study. *Nanomedicine* **2016**, *11*, nnm-2016-0248. doi:10.2217/nnm-2016-0248.
- [7679](#). Xuan, M.; Shao, J.; Zhao, J.; Li, Q.; Dai, L.; Li, J. Magnetic Mesoporous Silica Nanoparticles Cloaked by Red Blood Cell Membranes: Applications in Cancer Therapy. *Angew. Chemie - Int. Ed.* **2018**, *57*, 6049–6053. doi:10.1002/anie.201712996.
- [7780](#). Liu, M.-C.; Liu, B.; Chen, X.-L.; Lin, H.-C.; Sun, X.-Y.; Lu, J.-Z.; Li, Y.-Y.; Yan, S.-Q.; Zhang, L.-Y.; Zhao, P. Calcium carbonate end-capped, folate-mediated Fe₃O₄@mSiO₂ core-shell nanocarriers as targeted controlled-release drug delivery system. *J. Biomater. Appl.* **2018**, *32*, 1090–1104. doi:10.1177/0885328217752994.
- [7881](#). Singh, A.; Sahoo, S. K. Magnetic nanoparticles: a novel platform for cancer theranostics. *Drug Discov. Today* **2014**, *19*, 474–481. doi:10.1016/j.drudis.2013.10.005.
- [7982](#). Gobbo, O. L.; Sjaastad, K.; Radomski, M. W.; Volkov, Y.; Prina-Mello, A. Magnetic Nanoparticles in Cancer Theranostics. *Theranostics* **2015**, *5*, 1249–1263. doi:10.7150/thno.11544.
- [83](#). Ye, F.; Laurent, S.; Fornara, A.; Astolfi, L.; Qin, J.; Roch, A.; Martini, A.; Toprak, M. S.; Muller, R. N.; Muhammed, M. Uniform mesoporous silica coated iron oxide nanoparticles as a highly efficient, nontoxic MRI T2 contrast agent with tunable proton relaxivities. *Contrast Media Mol. Imaging* **2012**, *7*, 460–468. doi:10.1002/cmmi.1473.
- [84](#). Hurley, K. R.; Lin, Y.-S.; Zhang, J.; Egger, S. M.; Haynes, C. L. Effects of Mesoporous Silica Coating and Postsynthetic Treatment on the Transverse Relaxivity of Iron Oxide Nanoparticles. *Chem. Mater.* **2013**, *25*, 1968–1978. doi:10.1021/cm400711h.
- [8085](#). Giri, S.; Trewyn, B. G.; Stellmaker, M. P.; Lin, V. S.-Y. Stimuli-Responsive Controlled-Release Delivery System Based on Mesoporous Silica Nanorods Capped with Magnetic Nanoparticles. *Angew. Chemie Int. Ed.* **2005**, *44*, 5038–5044. doi:10.1002/anie.200501819.
- [8186](#). Lee, J. E.; Lee, N.; Kim, H.; Kim, J. H. J. H.; Choi, S. H.; Kim, T.; Song, I. C.; Park, S. P.; Moon, W. K.; Hyeon, T. Uniform mesoporous dye-doped silica nanocrystals for simultaneous enhanced magnetic resonance imaging, fluorescence imaging, and drug delivery. *J. Am. Chem. Soc.* **2010**, *132*, 552–557. doi:10.1021/ja905793q.
- [8287](#). Wang, D.; Lin, H.; Zhang, G.; Si, Y.; Yang, H.; Bai, G.; Yang, C.; Zhong, K.; Cai, D.; Wu, Z.; Wang, R.; Zou, D. Effective pH-Activated Theranostic Platform for Synchronous Magnetic Resonance Imaging Diagnosis and Chemotherapy. *ACS Appl. Mater. Interfaces* **2018**, *10*, 31114–31123. doi:10.1021/acsami.8b11408.
- [8388](#). Huang, G.; Liu, R.; Hu, Y.; Li, S.; Wu, Y.; Qiu, Y.; Li, J.; Yang, H.-H. FeOOH-loaded mesoporous silica nanoparticles as a theranostic platform with pH-responsive MRI contrast enhancement and drug release. *Sci. China Chem.* **2018**, *61*, 806–811. doi:10.1007/s11426-017-9217-4.

89. Carniato, F.; Tei, L.; Dastrù, W.; Marchese, L.; Botta, M. Relaxivity modulation in Gd-functionalised mesoporous silicas. *Chem. Commun.* **2009**, 1246–1248, doi:10.1039/b820591d.
90. Carniato, F.; Tei, L.; Cossi, M.; Marchese, L.; Botta, M. A Chemical Strategy for the Relaxivity Enhancement of GdIII Chelates Anchored on Mesoporous Silica Nanoparticles. *Chem. - A Eur. J.* **2010**, *16*, 10727–10734, doi:10.1002/chem.201000499.
91. Davis, J. J.; Huang, W.-Y.; Davies, G.-L. Location-tuned relaxivity in Gd-doped mesoporous silica nanoparticles. *J. Mater. Chem.* **2012**, *22*, 22848–28850, doi:10.1039/c2jm35116a.
92. Cao, M.; Wang, P.; Kou, Y.; Wang, J.; Liu, J.; Li, Y.; Li, J.; Wang, L.; Chen, C. Gadolinium(III)-Chelated Silica Nanospheres Integrating Chemotherapy and Photothermal Therapy for Cancer Treatment and Magnetic Resonance Imaging. *ACS Appl. Mater. Interfaces* **2015**, *7*, 25014–25023, doi:10.1021/acsami.5b06938.
93. Pavitra, E.; Seeta Rama Raju, G.; Nagaraju, G. P.; Nagaraju, G.; Han, Y.-K.; Huh, Y. S.; Yu, J. S. TPAOH assisted size-tunable Gd₂O₃@mSi core-shell nanostructures for multifunctional biomedical applications. *Chem. Commun.* **2018**, *54*, 747–750, doi:10.1039/C7CC07975C.
94. Zou, R.; Gong, S.; Shi, J.; Jiao, J.; Wong, K.-L.; Zhang, H.; Wang, J.; Su, Q. Magnetic-NIR Persistent Luminescent Dual-Modal ZGOCS@MSNs@Gd₂O₃ Core-Shell Nanoprobes For In Vivo Imaging. *Chem. Mater.* **2017**, *29*, 3938–3946, doi:10.1021/acs.chemmater.7b00087.
8495. Ren, S.; Yang, J.; Ma, L.; Li, X.; Wu, W.; Liu, C.; He, J.; Miao, L. Ternary-Responsive Drug Delivery with Activatable Dual Mode Contrast-Enhanced *in vivo* Imaging. *ACS Appl. Mater. Interfaces* **2018**, *10*, 31947–31958. doi:10.1021/acsami.8b10564.
8596. Shao, D.; Li, J.; Zheng, X.; Pan, Y.; Wang, Z.; Zhang, M.; Chen, Q. X.; Dong, W. F.; Chen, L. Janus “nano-bullets” for magnetic targeting liver cancer chemotherapy. *Biomaterials* **2016**, *100*, 118–133. doi:10.1016/j.biomaterials.2016.05.030.
8697. Wang, Z.; Chang, Z.; Lu, M.; Shao, D.; Yue, J.; Yang, D.; Zheng, X.; Li, M.; He, K.; Zhang, M.; Chen, L.; Dong, W. fei Shape-controlled magnetic mesoporous silica nanoparticles for magnetically-mediated suicide gene therapy of hepatocellular carcinoma. *Biomaterials* **2018**, *154*, 147–157. doi:10.1016/j.biomaterials.2017.10.047.
8798. Xing, H.; Wang, Z.; Shao, D.; Chang, Z.; Ge, M.; Li, L.; Wu, M.; Yan, Z.; Dong, W. Janus nanocarriers for magnetically targeted and hyperthermia-enhanced curcumin therapy of liver cancer. *RSC Adv.* **2018**, *8*, 30448–30454. doi:10.1039/C8RA05694C.
8899. Zhang, Y.; Yang, H.; Zhou, Z.; Huang, K.; Yang, S.; Han, G. Recent Advances on Magnetic Relaxation Switching Assay-Based Nanosensors. *Bioconjug. Chem.* **2017**, *28*, 869–879. doi:10.1021/acs.bioconjchem.7b00059.
89100. Lee, H.; Sun, E.; Ham, D.; Weissleder, R. Chip-NMR biosensor for detection and molecular analysis of cells. *Nat. Med.* **2008**, *14*, 869–874. doi:10.1038/nm.1711.
90101. Shelby, T.; Banerjee, T.; Zegar, I.; Santra, S. Highly Sensitive, Engineered Magnetic Nanosensors to Investigate the Ambiguous Activity of Zika Virus and Binding Receptors. *Sci. Rep.* **2017**, *7*, 7377. doi:10.1038/s41598-017-07620-y.
94102. Xie, L.; Jiang, R.; Zhu, F.; Liu, H.; Ouyang, G. Application of functionalized magnetic nanoparticles in sample preparation. *Anal. Bioanal. Chem.* **2014**, *406*, 377–399. doi:10.1007/s00216-013-7302-6.
92103. Li, Y.; Zhang, X.; Deng, C. Functionalized magnetic nanoparticles for sample preparation in proteomics and peptidomics analysis. *Chem. Soc. Rev.* **2013**, *42*, 8517–8539. doi:10.1039/c3cs60156k.
93104. Lee, M. S.; Su, C.-M.; Yeh, J.-C.; Wu, P.-R.; Tsai, T.-Y.; Lou, S.-L. Synthesis of composite magnetic nanoparticles Fe₃O₄ with alendronate for osteoporosis treatment. *Int. J. Nanomedicine* **2016**, Volume 11, 4583–4594. doi:10.2147/IJN.S112415.
94105. Wan, L.; Song, H.; Chen, X.; Zhang, Y.; Yue, Q.; Pan, P.; Su, J.; Elzatahry, A. A.; Deng, Y. A

- 1135 Magnetic-Field Guided Interface Coassembly Approach to Magnetic Mesoporous Silica
1136 Nanochains for Osteoclast-Targeted Inhibition and Heterogeneous Nanocatalysis. *Adv.*
1137 *Mater.* **2018**, *30*, 1–9. doi:10.1002/adma.201707515.
- 1138 | [95106](#). Jaque, D.; Martínez Maestro, L.; del Rosal, B.; Haro-Gonzalez, P.; Benayas, A.; Plaza, J. L.;
1139 Martín Rodríguez, E.; García Solé, J. Nanoparticles for photothermal therapies. *Nanoscale*
1140 **2014**, *6*, 9494–9530. doi:10.1039/C4NR00708E.
- 1141 | [96107](#). Sortino, S. *Light-Responsive Nanostructured Systems for Applications in Nanomedicine*; 2016; Vol.
1142 370; ISBN 978-3-319-22941-6.
- 1143 | [97108](#). Lucky, S. S.; Soo, K. C.; Zhang, Y. Nanoparticles in photodynamic therapy. *Chem. Rev.* **2015**,
1144 *115*, 1990–2042. doi:10.1021/cr5004198.
- 1145 | [98109](#). Liu, Z.; Robinson, J. T.; Tabakman, S. M.; Yang, K.; Dai, H. Carbon materials for drug delivery
1146 & cancer therapy. *Mater. Today* **2011**, *14*, 316–323. doi:10.1016/S1369-7021(11)70161-4.
- 1147 | [99110](#). Xu, L.; Cheng, L.; Wang, C.; Peng, R.; Liu, Z. Conjugated polymers for photothermal therapy
1148 of cancer. *Polym. Chem.* **2014**, *5*, 1573–1580. doi:10.1039/C3PY01196H.
- 1149 | [400111](#). Chen, J.; Wiley, B.; Li, Z.-Y.; Campbell, D.; Saeki, F.; Cang, H.; Au, L.; Lee, J.; Li, X.; Xia, Y.
1150 Gold Nanocages: Engineering Their Structure for Biomedical Applications. *Adv. Mater.* **2005**,
1151 *17*, 2255–2261. doi:10.1002/adma.200500833.
- 1152 | [401112](#). Zhao, T.; Chen, L.; Li, Q.; Li, X. Near-infrared light triggered drug release from
1153 mesoporous silica nanoparticles. *J. Mater. Chem. B* **2018**, *6*, 7112–7121.
1154 doi:10.1039/C8TB01548A.
- 1155 | [402113](#). Spagnul, C.; Turner, L. C.; Boyle, R. W. Immobilized photosensitizers for antimicrobial
1156 applications. *J. Photochem. Photobiol. B Biol.* **2015**, *150*, 11–30.
1157 doi:10.1016/j.jphotobiol.2015.04.021.
- 1158 | [403114](#). Kwiatkowski, S.; Knap, B.; Przystupski, D.; Saczko, J.; Kędzierska, E.; Knap-Czop, K.;
1159 Kotlińska, J.; Michel, O.; Kotowski, K.; Kulbacka, J. Photodynamic therapy – mechanisms,
1160 photosensitizers and combinations. *Biomed. Pharmacother.* **2018**, *106*, 1098–1107.
1161 doi:10.1016/j.biopha.2018.07.049.
- 1162 | [404115](#). Patel, K.; Raj, B. S.; Chen, Y.; Lou, X. Novel folic acid conjugated Fe₃O₄-ZnO hybrid
1163 nanoparticles for targeted photodynamic therapy. *Colloids Surfaces B Biointerfaces* **2017**, *150*,
1164 317–325. doi:10.1016/j.colsurfb.2016.10.045.
- 1165 | [405116](#). Lucky, S. S.; Muhammad Idris, N.; Li, Z.; Huang, K.; Soo, K. C.; Zhang, Y. Titania Coated
1166 Upconversion Nanoparticles for Near-Infrared Light Triggered Photodynamic Therapy. *ACS*
1167 *Nano* **2015**, *9*, 191–205. doi:10.1021/nn503450t.
- 1168 | [406117](#). Hackenberg, S.; Scherzed, A.; Kessler, M.; Froelich, K.; Ginzkey, C.; Koehler, C.; Burghartz,
1169 M.; Hagen, R.; Kleinsasser, N. Zinc oxide nanoparticles induce photocatalytic cell death in
1170 human head and neck squamous cell carcinoma cell lines *in vitro*. *Int. J. Oncol.* **2010**, *37*, 1583–
1171 1590. doi:10.3892/ijo_00000812.
- 1172 | [407118](#). Li, J.; Guo, D.; Wang, X.; Wang, H.; Jiang, H.; Chen, B. The Photodynamic Effect of
1173 Different Size ZnO Nanoparticles on Cancer Cell Proliferation *In vitro*. *Nanoscale Res. Lett.*
1174 **2010**, *5*, 1063–1071. doi:10.1007/s11671-010-9603-4.
- 1175 | [408119](#). Li, Y.; Lu, W.; Huang, Q.; Li, C.; Chen, W. Copper sulfide nanoparticles for photothermal
1176 ablation of tumor cells. *Nanomedicine* **2010**, *5*, 1161–1171. doi:10.2217/nnm.10.85.
- 1177 | [409120](#). Wang, S.; Riedinger, A.; Li, H.; Fu, C.; Liu, H.; Li, L.; Liu, T.; Tan, L.; Barthel, M. J.; Pugliese,
1178 G.; De Donato, F.; Scotto D'Abbusco, M.; Meng, X.; Manna, L.; Meng, H.; Pellegrino, T.
1179 Plasmonic Copper Sulfide Nanocrystals Exhibiting Near-Infrared Photothermal and
1180 Photodynamic Therapeutic Effects. *ACS Nano* **2015**, *9*, 1788–1800. doi:10.1021/nn506687t.
- 1181 | [410121](#). Espinosa, A.; Di Corato, R.; Kolosnjaj-Tabi, J.; Flaud, P.; Pellegrino, T.; Wilhelm, C. Duality
1182 of Iron Oxide Nanoparticles in Cancer Therapy: Amplification of Heating Efficiency by
1183 Magnetic Hyperthermia and Photothermal Bimodal Treatment. *ACS Nano* **2016**, *10*, 2436–
1184 2446. doi:10.1021/acsnano.5b07249.
- 1185 | [411122](#). Hu, Y.; Hu, H.; Yan, J.; Zhang, C.; Li, Y.; Wang, M.; Tan, W.; Liu, J.; Pan, Y. Multifunctional
1186 Porous Iron Oxide Nanoagents for MRI and Photothermal/Chemo Synergistic Therapy.

- 1187 *Bioconj. Chem.* **2018**, *29*, 1283–1290. doi:10.1021/acs.bioconjchem.8b00052.
- 1188 | [412123](#). Zhang, Z.; Wang, L.; Wang, J.; Jiang, X.; Li, X.; Hu, Z.; Ji, Y.; Wu, X.; Chen, C. Mesoporous
1189 Silica-Coated Gold Nanorods as a Light-Mediated Multifunctional Theranostic Platform for
1190 Cancer Treatment. *Adv. Mater.* **2012**, *24*, 1418–1423. doi:10.1002/adma.201104714.
- 1191 | [413124](#). Zhang, T.; Ding, Z.; Lin, H.; Cui, L.; Yang, C.; Li, X.; Niu, H.; An, N.; Tong, R.; Qu, F.
1192 pH-Sensitive Gold Nanorods with a Mesoporous Silica Shell for Drug Release and
1193 Photothermal Therapy. *Eur. J. Inorg. Chem.* **2015**, *2015*, 2277–2284. doi:10.1002/ejic.201403247.
- 1194 | [444125](#). Liu, Y.; Xu, M.; Chen, Q.; Guan, G.; Hu, W.; Zhao, X.; Qiao, M.; Hu, H.; Liang, Y.; Zhu, H.;
1195 Chen, D. Gold nanorods/mesoporous silica-based nanocomposite as theranostic agents for
1196 targeting near-infrared imaging and photothermal therapy induced with laser. *Int. J.*
1197 *Nanomedicine* **2015**, *10*, 4747–4761. doi:10.2147/IJN.S82940.
- 1198 | [415126](#). Liu, J.; Detrembleur, C.; De Pauw-Gillet, M. C.; Mornet, S.; Jérôme, C.; Duguet, E. Gold
1199 nanorods coated with mesoporous silica shell as drug delivery system for remote near
1200 infrared light-activated release and potential phototherapy. *Small* **2015**, *11*, 2323–2332.
1201 doi:10.1002/smll.201402145.
- 1202 | [416127](#). Villaverde, G.; Gómez-Graña, S.; Guisasola, E.; García, I.; Hanske, C.; Liz-Marzán, L. M.;
1203 Baeza, A.; Vallet-Regí, M. Targeted Chemo-Photothermal Therapy: A Nanomedicine
1204 Approximation to Selective Melanoma Treatment. *Part. Part. Syst. Character.* **2018**, *35*, 1800148.
1205 doi:10.1002/ppsc.201800148.
- 1206 | [417128](#). Moreira, A. F.; Rodrigues, C. F.; Reis, C. A.; Costa, E. C.; Correia, I. J. Gold-core silica shell
1207 nanoparticles application in imaging and therapy: A review. *Microporous Mesoporous Mater.*
1208 **2018**, *270*, 168–179. doi:10.1016/j.micromeso.2018.05.022.
- 1209 | [418129](#). Zhang, L.; Chen, Y.; Li, Z.; Li, L.; Saint-Cricq, P.; Li, C.; Lin, J.; Wang, C.; Su, Z.; Zink, J. I.
1210 Tailored Synthesis of Octopus-type Janus Nanoparticles for Synergistic Actively-Targeted
1211 and Chemo-Photothermal Therapy. *Angew. Chemie Int. Ed.* **2016**, *55*, 2118–2121.
1212 doi:10.1002/anie.201510409.
- 1213 | [419130](#). Hernández Montoto, A.; Montes, R.; Samadi, A.; Gorbe, M.; Terrés, J. M.; Cao-Milán, R.;
1214 Aznar, E.; Ibañez, J.; Masot, R.; Marcos, M. D.; Orzáez, M.; Sancenón, F.; Oddershede, L. B.;
1215 Martínez-Máñez, R. Gold Nanostars Coated with Mesoporous Silica Are Effective and
1216 Nontoxic Photothermal Agents Capable of Gate Keeping and Laser-Induced Drug Release.
1217 *ACS Appl. Mater. Interfaces* **2018**, *10*, 27644–27656. doi:10.1021/acsami.8b08395.
- 1218 | [420131](#). Raghavan, V.; O'Flatharta, C.; Dwyer, R.; Breathnach, A.; Zafar, H.; Dockery, P.; Wheatley,
1219 A.; Keogh, I.; Leahy, M.; Olivo, M. Dual plasmonic gold nanostars for photoacoustic imaging
1220 and photothermal therapy. *Nanomedicine* **2017**, *12*, 457–471. doi:10.2217/nnm-2016-0318.
- 1221 | [421132](#). Castillo, R. R.; Hernández-Escobar, D.; Gómez-Graña, S.; Vallet-Regí, M. Reversible
1222 Nanogate System for Mesoporous Silica Nanoparticles Based on Diels-Alder Adducts. *Chem.*
1223 *- A Eur. J.* **2018**, *24*, 6992–7001. doi:10.1002/chem.201706100.
- 1224 | [422133](#). Li, X.; Xing, L.; Zheng, K.; Wei, P.; Du, L.; Shen, M.; Shi, X. Formation of Gold
1225 Nanostar-Coated Hollow Mesoporous Silica for Tumor Multimodality Imaging and
1226 Photothermal Therapy. *ACS Appl. Mater. Interfaces* **2017**, *9*, 5817–5827.
1227 doi:10.1021/acsami.6b15185.
- 1228 | [423134](#). Singhana, B.; Slattery, P.; Chen, A.; Wallace, M.; Melancon, M. P. Light-Activatable Gold
1229 Nanoshells for Drug Delivery Applications. *AAPS PharmSciTech* **2014**, *15*, 741–752.
1230 doi:10.1208/s12249-014-0097-8.
- 1231 | [424135](#). Paithankar, D.; Hwang, B. H.; Munavalli, G.; Kauvar, A.; Lloyd, J.; Blomgren, R.; Faupel, L.;
1232 Meyer, T.; Mitragotri, S. Ultrasonic delivery of silica-gold nanoshells for photothermolysis of
1233 sebaceous glands in humans: Nanotechnology from the bench to clinic. *J. Control. Release*
1234 **2015**, *206*, 30–36. doi:10.1016/j.jconrel.2015.03.004.
- 1235 | [425136](#). Wang, H.; Zhao, R.; Li, Y.; Liu, H.; Li, F.; Zhao, Y.; Nie, G. Aspect ratios of gold nanoshell
1236 capsules mediated melanoma ablation by synergistic photothermal therapy and
1237 chemotherapy. *Nanomedicine Nanotechnology, Biol. Med.* **2016**, *12*, 439–448.
1238 doi:10.1016/j.nano.2015.11.013.

- 1239 | [426137](#). He, C.-F.; Wang, S.-H.; Yu, Y.-J.; Shen, H.-Y.; Zhao, Y.; Gao, H.-L.; Wang, H.; Li, L.-L.; Liu,
1240 | H.-Y.; He, C.-F.; Wang, S.-H.; Yu, Y.-J.; Shen, H.-Y.; Zhao, Y.; Gao, H.-L.; Wang, H.; Li, L.-L.;
1241 | Liu, H.-Y. Advances in biodegradable nanomaterials for photothermal therapy of cancer.
1242 | *Cancer Biol. Med.* **2016**, *13*, 299–312. doi:10.20892/j.issn.2095-3941.2016.0052.
- 1243 | [427138](#). Song, G.; Wang, Q.; Wang, Y.; Lv, G.; Li, C.; Zou, R.; Chen, Z.; Qin, Z.; Huo, K.; Hu, R.; Hu,
1244 | J. A low-toxic multifunctional nanoplatform based on Cu₉S₅@mSiO₂ core-shell
1245 | nanocomposites: Combining photothermal- and chemotherapies with infrared thermal
1246 | imaging for cancer treatment. *Adv. Funct. Mater.* **2013**, *23*, 4281–4292.
1247 | doi:10.1002/adfm.201203317.
- 1248 | [428139](#). Lu, F.; Wang, J.; Yang, L.; Zhu, J. J. A facile one-pot synthesis of colloidal stable,
1249 | monodisperse, highly PEGylated CuS@ mSiO₂ nanocomposites for the combination of
1250 | photothermal therapy and chemotherapy. *Chem. Commun.* **2015**, *51*, 9447–9450.
1251 | doi:10.1039/c5cc01725d.
- 1252 | [429140](#). Zhang, Y.; Hou, Z.; Ge, Y.; Deng, K.; Liu, B.; Li, X.; Li, Q.; Cheng, Z.; Ma, P.; Li, C.; Lin, J.
1253 | DNA-Hybrid-Gated Photothermal Mesoporous Silica Nanoparticles for NIR-Responsive and
1254 | Aptamer-Targeted Drug Delivery. *ACS Appl. Mater. Interfaces* **2015**, *7*, 20696–20706.
1255 | doi:10.1021/acsami.5b05522.
- 1256 | [430141](#). Castillo, R. R.; Baeza, A.; Vallet-Regí, M. Recent applications of the combination of
1257 | mesoporous silica nanoparticles with nucleic acids: development of bioresponsive devices,
1258 | carriers and sensors. *Biomater. Sci.* **2017**, *5*, 353–377. doi:10.1039/C6BM00872K.
- 1259 | [431142](#). Su, X.; Zhao, F.; Wang, Y.; Yan, X.; Jia, S.; Du, B. CuS as a gatekeeper of mesoporous
1260 | upconversion nanoparticles-based drug controlled release system for tumor-targeted
1261 | multimodal imaging and synergetic chemo-thermotherapy. *Nanomedicine Nanotechnology,*
1262 | *Biol. Med.* **2017**, *13*, 1761–1772. doi:10.1016/j.nano.2017.03.008.
- 1263 | [143](#). Liu, X.; Yang, T.; Han, Y.; Zou, L.; Yang, H.; Jiang, J.; Liu, S.; Zhao, Q.; Huang, W. *In Situ*
1264 | *Growth of CuS/SiO₂-Based Multifunctional Nanotherapeutic Agents for Combined*
1265 | *Photodynamic/Photothermal Cancer Therapy. ACS Appl. Mater. Interfaces* **2018**, *10*, 31008–
1266 | [31018](#), doi:10.1021/acsami.8b10339.
- 1267 | [432144](#). Lee, D. S.; Im, H.-J.; Lee, Y.-S. Radionanomedicine: Widened perspectives of molecular
1268 | theragnosis. *Nanomedicine Nanotechnology, Biol. Med.* **2015**, *11*, 795–810.
1269 | doi:10.1016/j.nano.2014.12.010.
- 1270 | [433145](#). Ni, D.; Jiang, D.; Ehlerding, E. B.; Huang, P.; Cai, W. Radiolabeling Silica-Based
1271 | Nanoparticles via Coordination Chemistry: Basic Principles, Strategies, and Applications.
1272 | *Acc. Chem. Res.* **2018**, *51*, 778–788. doi:10.1021/acs.accounts.7b00635.
- 1273 | [434146](#). Chen, F.; Hong, H.; Goel, S.; Graves, S. A.; Orbay, H.; Ehlerding, E. B.; Shi, S.; Theuer, C. P.;
1274 | Nickles, R. J.; Cai, W. *In vivo* Tumor Vasculature Targeting of CuS@MSN Based Theranostic
1275 | Nanomedicine. *ACS Nano* **2015**, *9*, 3926–3934. doi:10.1021/nn507241v.
- 1276 | [147](#). Estelrich, J.; Busquets, M. A. *Iron Oxide Nanoparticles in Photothermal Therapy. Molecules*
1277 | **2018**, *23*, 1567. doi: 10.3390/molecules23071567.
- 1278 | [435148](#). Bobo, D.; Robinson, K. J.; Islam, J.; Thurecht, K. J.; Corrie, S. R. Nanoparticle-Based
1279 | Medicines: A Review of FDA-Approved Materials and Clinical Trials to Date. *Pharm. Res.*
1280 | **2016**, *33*, 2373–2387. doi:10.1007/s11095-016-1958-5.
- 1281 | [436149](#). Caster, J. M.; Patel, A. N.; Zhang, T.; Wang, A. Investigational nanomedicines in 2016: a
1282 | review of nanotherapeutics currently undergoing clinical trials. *Wiley Interdiscip. Rev.*
1283 | *Nanomedicine Nanobiotechnology* **2017**, *9*, e1416. doi:10.1002/wnan.1416.
- 1284 | [437150](#). Wu, W.-C.; Tracy, J. B. Large-Scale Silica Overcoating of Gold Nanorods with Tunable Shell
1285 | Thicknesses. *Chem. Mater.* **2015**, *27*, 2888–2894. doi:10.1021/cm504764v.
- 1286 | [438151](#). Rowe, L. R.; Chapman, B. S.; Tracy, J. B. Understanding and Controlling the Morphology of
1287 | Silica Shells on Gold Nanorods. *Chem. Mater.* **2018**, *30*, 6249–6258.
1288 | doi:10.1021/acs.chemmater.8b00794.
- 1289 | [439152](#). Ali, M. R. K.; Rahman, M. A.; Wu, Y.; Han, T.; Peng, X.; Mackey, M. A.; Wang, D.; Shin, H.
1290 | J.; Chen, Z. G.; Xiao, H.; Wu, R.; Tang, Y.; Shin, D. M.; El-Sayed, M. A. Efficacy, long-term

- 1291 toxicity, and mechanistic studies of gold nanorods photothermal therapy of cancer in
 1292 xenograft mice. *Proc. Natl. Acad. Sci.* **2017**, *114*, E3110–E3118. doi:10.1073/pnas.1619302114.
- 1293 | [440153](#). Aioub, M.; Panikkanvalappil, S. R.; El-Sayed, M. A. Platinum-Coated Gold Nanorods:
 1294 Efficient Reactive Oxygen Scavengers That Prevent Oxidative Damage toward Healthy,
 1295 Untreated Cells during Plasmonic Photothermal Therapy. *ACS Nano* **2017**, *11*, 579–586.
 1296 doi:10.1021/acsnano.6b06651.
- 1297 | [441154](#). Lin, S.; Wang, Y.; Chen, Z.; Li, L.; Zeng, J.; Dong, Q.; Wang, Y.; Chai, Z. Biomineralized
 1298 Enzyme-Like Cobalt Sulfide Nanodots for Synergetic Phototherapy with Tumor Multimodal
 1299 Imaging Navigation. *ACS Sustain. Chem. Eng.* **2018**, *6*, 12061–12069.
 1300 doi:10.1021/acssuschemeng.8b02386.
- 1301 | [442155](#). Croissant, J. G.; Zink, J. I.; Raehm, L.; Durand, J. O. Two-Photon-Excited Silica and
 1302 Organosilica Nanoparticles for Spatiotemporal Cancer Treatment. *Adv. Healthc. Mater.* **2018**,
 1303 *7*, 1–22. doi:10.1002/adhm.201701248.
- 1304 | [443156](#). Bayir, S.; Barras, A.; Boukherroub, R.; Szunerits, S.; Raehm, L.; Richeter, S.; Durand, J.-O.
 1305 Mesoporous silica nanoparticles in recent photodynamic therapy applications. *Photochem.*
 1306 *Photobiol. Sci.* **2018**, *17*, 1651–1674. doi:10.1039/C8PP00143J.
- 1307 | [444157](#). Wolfbeis, O. S. An overview of nanoparticles commonly used in fluorescent bioimaging.
 1308 *Chem. Soc. Rev.* **2015**, *44*, 4743–4768. doi:10.1039/C4CS00392F.
- 1309 | [445158](#). Wang, F.; Liu, X. Recent advances in the chemistry of lanthanide-doped upconversion
 1310 nanocrystals. *Chem. Soc. Rev.* **2009**, *38*, 976–989. doi:10.1039/b809132n.
- 1311 | [446159](#). Zhu, S.; Gu, Z. Lanthanide-doped materials as dual imaging and therapeutic agents. In
 1312 *Lanthanide-Based Multifunctional Materials*; Elsevier, 2018; pp. 381–410 ISBN 9780128138403.
- 1313 | [447160](#). Wen, S.; Zhou, J.; Zheng, K.; Bednarkiewicz, A.; Liu, X.; Jin, D. Advances in highly doped
 1314 upconversion nanoparticles. *Nat. Commun.* **2018**, *9*, 2415. doi:10.1038/s41467-018-04813-5.
- 1315 | [448161](#). Lim, S. Y.; Shen, W.; Gao, Z. Carbon quantum dots and their applications. *Chem. Soc. Rev.*
 1316 **2015**, *44*, 362–381. doi:10.1039/C4CS00269E.
- 1317 | [449162](#). Wang, Z.; Zeng, H.; Sun, L. Graphene quantum dots: versatile photoluminescence for
 1318 energy, biomedical, and environmental applications. *J. Mater. Chem. C* **2015**, *3*, 1157–1165.
 1319 doi:10.1039/C4TC02536A.
- 1320 | [450163](#). Zheng, X. T.; Ananthanarayanan, A.; Luo, K. Q.; Chen, P. Glowing Graphene Quantum
 1321 Dots and Carbon Dots: Properties, Syntheses, and Biological Applications. *Small* **2015**, *11*,
 1322 1620–1636. doi:10.1002/sml.201402648.
- 1323 | [451164](#). Wegner, K. D.; Hildebrandt, N. Quantum dots: bright and versatile *in vitro* and *in vivo*
 1324 fluorescence imaging biosensors. *Chem. Soc. Rev.* **2015**, *44*, 4792–4834.
 1325 doi:10.1039/C4CS00532E.
- 1326 | [452165](#). Pu, Y.; Cai, F.; Wang, D.; Wang, J.-X.; Chen, J.-F. Colloidal Synthesis of Semiconductor
 1327 Quantum Dots toward Large-Scale Production: A Review. *Ind. Eng. Chem. Res.* **2018**, *57*, 1790–
 1328 1802. doi:10.1021/acs.iecr.7b04836.
- 1329 | [453166](#). Gnach, A.; Lipinski, T.; Bednarkiewicz, A.; Rybka, J.; Capobianco, J. A. Upconverting
 1330 nanoparticles: assessing the toxicity. *Chem. Soc. Rev.* **2015**, *44*, 1561–1584.
 1331 doi:10.1039/C4CS00177J.
- 1332 | [454167](#). Rocha, T. L.; Mestre, N. C.; Sabóia-Morais, S. M. T.; Bebianno, M. J. Environmental
 1333 behaviour and ecotoxicity of quantum dots at various trophic levels: A review. *Environ. Int.*
 1334 **2017**, *98*, 1–17. doi:10.1016/j.envint.2016.09.021.
- 1335 | [455168](#). Oh, E.; Liu, R.; Nel, A.; Gemill, K. B.; Bilal, M.; Cohen, Y.; Medintz, I. L. Meta-analysis of
 1336 cellular toxicity for cadmium-containing quantum dots. *Nat. Nanotechnol.* **2016**, *11*, 479–486.
 1337 doi:10.1038/nnano.2015.338.
- 1338 | [456169](#). Massey, M.; Wu, M.; Conroy, E. M.; Algar, W. R. Mind your P's and Q's: the coming of age
 1339 of semiconducting polymer dots and semiconductor quantum dots in biological applications.
 1340 *Curr. Opin. Biotechnol.* **2015**, *34*, 30–40. doi:10.1016/j.copbio.2014.11.006.
- 1341 | [457170](#). Pagano, G.; Guida, M.; Tommasi, F.; Oral, R. Health effects and toxicity mechanisms of rare
 1342 earth elements—Knowledge gaps and research prospects. *Ecotoxicol. Environ. Saf.* **2015**, *115*,

- 1343 40–48. doi:10.1016/j.ecoenv.2015.01.030.
- 1344 | [458171](#). Rogosnitzky, M.; Branch, S. Gadolinium-based contrast agent toxicity: a review of known
1345 and proposed mechanisms. *BioMetals* **2016**, *29*, 365–376. doi:10.1007/s10534-016-9931-7.
- 1346 | [459172](#). *Fluorine: Chemistry, Analysis, Function and Effects (Chapter 4: Fluoride Metabolism)*; Preedy, V.
1347 R., Ed.; Food and Nutritional Components in Focus; Royal Society of Chemistry: Cambridge,
1348 2015; ISBN 978-1-84973-888-0.
- 1349 | [460173](#). Phillips, E.; Penate-Medina, O.; Zanzonico, P. B.; Carvajal, R. D.; Mohan, P.; Ye, Y.; Humm,
1350 J.; Gonen, M.; Kalaigian, H.; Schoder, H.; Strauss, H. W.; Larson, S. M.; Wiesner, U.; Bradbury,
1351 M. S. Clinical translation of an ultrasmall inorganic optical-PET imaging nanoparticle probe.
1352 *Sci. Transl. Med.* **2014**, *6*, 260ra149. doi:10.1126/scitranslmed.3009524.
- 1353 | [461174](#). Zhou, J.; Yang, Y.; Zhang, C. Toward Biocompatible Semiconductor Quantum Dots: From
1354 Biosynthesis and Bioconjugation to Biomedical Application. *Chem. Rev.* **2015**, *115*, 11669–
1355 11717. doi:10.1021/acs.chemrev.5b00049.
- 1356 | [462175](#). Biermann, A.; Aubert, T.; Baumeister, P.; Drijvers, E.; Hens, Z.; Maultzsch, J. Interface
1357 formation during silica encapsulation of colloidal CdSe/CdS quantum dots observed by in
1358 situ Raman spectroscopy. *J. Chem. Phys.* **2017**, *146*, 134708. doi:10.1063/1.4979515.
- 1359 | [463176](#). Liu, Z.; Zhang, Y.; Fan, Y.; Chen, Z.; Tang, Z.; Zhao, J.; Lv, Y.; Lin, J.; Guo, X.; Zhang, J.; Liu,
1360 X. Toward Highly Luminescent and Stabilized Silica-Coated Perovskite Quantum Dots
1361 through Simply Mixing and Stirring under Room Temperature in Air. *ACS Appl. Mater.*
1362 *Interfaces* **2018**, *10*, 13053–13061. doi:10.1021/acsami.7b18964.
- 1363 | [464177](#). Li, H.; Li, Y.; Cheng, J. Molecularly Imprinted Silica Nanospheres Embedded CdSe
1364 Quantum Dots for Highly Selective and Sensitive Optosensing of Pyrethroids. *Chem. Mater.*
1365 **2010**, *22*, 2451–2457. doi:10.1021/cm902856y.
- 1366 | [465178](#). Hu, X.; Zrazhevskiy, P.; Gao, X. Encapsulation of Single Quantum Dots with Mesoporous
1367 Silica. *Ann. Biomed. Eng.* **2009**, *37*, 1960–1966. doi:10.1007/s10439-009-9660-y.
- 1368 | [466179](#). Zhang, K. Y.; Yu, Q.; Wei, H.; Liu, S.; Zhao, Q.; Huang, W. Long-Lived Emissive Probes for
1369 Time-Resolved Photoluminescence Bioimaging and Biosensing. *Chem. Rev.* **2018**, *118*, 1770–
1370 1839. doi:10.1021/acs.chemrev.7b00425.
- 1371 | [467180](#). Wu, J.; Kwon, B.; Liu, W.; Anslyn, E. V.; Wang, P.; Kim, J. S. Chromogenic/Fluorogenic
1372 Ensemble Chemosensing Systems. *Chem. Rev.* **2015**, *115*, 7893–7943. doi:10.1021/cr500553d.
- 1373 | [468181](#). Yu, L.; Lin, H.; Lu, X.; Chen, Y. Multifunctional Mesoporous Silica Nanoprobes: Material
1374 Chemistry-Based Fabrication and Bio-Imaging Functionality. *Av. Ther.* **2018**, *1*, 1800078.
1375 doi:10.1002/adtp.201800078.
- 1376 | [469182](#). Xu, G.; Zeng, S.; Zhang, B.; Swihart, M. T.; Yong, K.-T.; Prasad, P. N. New Generation
1377 Cadmium-Free Quantum Dots for Biophotonics and Nanomedicine. *Chem. Rev.* **2016**, *116*,
1378 12234–12327. doi:10.1021/acs.chemrev.6b00290.
- 1379 | [470183](#). Zhang, Z.; Shikha, S.; Liu, J.; Zhang, J.; Mei, Q.; Zhang, Y. Upconversion Nanoprobes:
1380 Recent Advances in Sensing Applications. *Anal. Chem.* **2019**, *91*, 548–568.
1381 doi:10.1021/acs.analchem.8b04049.
- 1382 | [471184](#). Duan, C.; Liang, L.; Li, L.; Zhang, R.; Xu, Z. P. Recent progress in upconversion
1383 luminescence nanomaterials for biomedical applications. *J. Mater. Chem. B* **2018**, *6*, 192–209.
1384 doi:10.1039/C7TB02527K.
- 1385 | [472185](#). Gulzar, A.; Xu, J.; Yang, P.; He, F.; Xu, L. Upconversion processes: versatile biological
1386 applications and biosafety. *Nanoscale* **2017**, *9*, 12248–12282. doi:10.1039/C7NR01836C.
- 1387 | [473186](#). Idris, N. M.; Gnanasammandhan, M. K.; Zhang, J.; Ho, P. C.; Mahendran, R.; Zhang, Y. *In*
1388 *vivo* photodynamic therapy using upconversion nanoparticles as remote-controlled
1389 nanotransducers. *Nat. Med.* **2012**, *18*, 1580–1585. doi:10.1038/nm.2933.
- 1390 | [474187](#). Gao, C.; Lin, Z.; Wu, Z.; Lin, X.; He, Q. Stem-Cell-Membrane Camouflaging on
1391 Near-Infrared Photoactivated Upconversion Nanoarchitectures for *in vivo*
1392 Remote-Controlled Photodynamic Therapy. *ACS Appl. Mater. Interfaces* **2016**, *8*, 34252–34260.
1393 doi:10.1021/acsami.6b12865.
- 1394 | [475188](#). Liu, Y.; Liu, Y.; Bu, W.; Cheng, C.; Zuo, C.; Xiao, Q.; Sun, Y.; Ni, D.; Zhang, C.; Liu, J.; Shi, J.

- Hypoxia Induced by Upconversion-Based Photodynamic Therapy: Towards Highly Effective Synergistic Bioreductive Therapy in Tumors. *Angew. Chemie* **2015**, *127*, 8223–8227. doi:10.1002/ange.201500478.
- [476189](#). Liu, J.; Bu, W.; Pan, L.; Shi, J. NIR-Triggered Anticancer Drug Delivery by Upconverting Nanoparticles with Integrated Azobenzene-Modified Mesoporous Silica. *Angew. Chemie Int. Ed.* **2013**, *52*, 4375–4379. doi:10.1002/anie.201300183.
- [477190](#). Dong, J.; Zink, J. I. Light or Heat? the Origin of Cargo Release from Nanoimpeller Particles Containing Upconversion Nanocrystals under IR Irradiation. *Small* **2015**, *11*, 4165–4172. doi:10.1002/smll.201500607.
- [478191](#). Han, R.; Shi, J.; Liu, Z.; Wang, H.; Wang, Y. Fabrication of Mesoporous-Silica-Coated Upconverting Nanoparticles with Ultrafast Photosensitizer Loading and 808 nm NIR-Light-Triggering Capability for Photodynamic Therapy. *Chem. - An Asian J.* **2017**, *12*, 2197–2201. doi:10.1002/asia.201700836.
- [479192](#). Jain, A.; Koyani, R.; Muñoz, C.; Sengar, P.; Contreras, O. E.; Juárez, P.; Hirata, G. A. Magnetic-luminescent cerium-doped gadolinium aluminum garnet nanoparticles for simultaneous imaging and photodynamic therapy of cancer cells. *J. Colloid Interface Sci.* **2018**, *526*, 220–229. doi:10.1016/j.jcis.2018.04.100.
- [480193](#). Gao, Z.; Liu, X.; Deng, G.; Zhou, F.; Zhang, L.; Wang, Q.; Lu, J. Fe₃O₄@mSiO₂-FA-CuS-PEG nanocomposites for magnetic resonance imaging and targeted chemo-photothermal synergistic therapy of cancer cells. *Dalt. Trans.* **2016**, *45*, 13456–13465. doi:10.1039/c6dt01714b.
- [481194](#). Yao, X.; Niu, X.; Ma, K.; Huang, P.; Grothe, J.; Kaskel, S.; Zhu, Y. Graphene Quantum Dots-Capped Magnetic Mesoporous Silica Nanoparticles as a Multifunctional Platform for Controlled Drug Delivery, Magnetic Hyperthermia, and Photothermal Therapy. *Small* **2017**, *13*, 1–11. doi:10.1002/smll.201602225.
- [482195](#). Sanavio, B.; Stellacci, F. Recent Advances in the Synthesis and Applications of Multimodal Gold-Iron Nanoparticles. *Curr. Med. Chem.* **2017**, *24*, 497–511. doi:10.2174/0929867323666160829111531.
- [483196](#). Yang, H.; Chen, Y.; Chen, Z.; Geng, Y.; Xie, X.; Shen, X.; Li, T.; Li, S.; Wu, C.; Liu, Y. Chemo-photodynamic combined gene therapy and dual-modal cancer imaging achieved by pH-responsive alginate/chitosan multilayer-modified magnetic mesoporous silica nanocomposites. *Biomater. Sci.* **2017**, *5*, 1001–1013. doi:10.1039/c7bm00043j.
- [484197](#). Sánchez, A.; Ovejero Paredes, K.; Ruiz-Cabello, J.; Martínez-Ruiz, P.; Pingarrón, J. M.; Villalonga, R.; Filice, M. Hybrid Decorated Core@Shell Janus Nanoparticles as a Flexible Platform for Targeted Multimodal Molecular Bioimaging of Cancer. *ACS Appl. Mater. Interfaces* **2018**, *10*, 31032–31043. doi:10.1021/acsami.8b10452.
- [485198](#). Qiu, H.; Cui, B.; Li, G.; Yang, J.; Peng, H.; Wang, Y.; Li, N.; Gao, R.; Chang, Z.; Wang, Y. Novel Fe₃O₄@ZnO@mSiO₂ Nanocarrier for targeted drug delivery and controllable release with microwave irradiation. *J. Phys. Chem. C* **2014**, *118*, 14929–14937. doi:10.1021/jp502820r.
- [486199](#). Xiao, Q.; Zheng, X.; Bu, W.; Ge, W.; Zhang, S.; Chen, F.; Xing, H.; Ren, Q.; Fan, W.; Zhao, K.; Hua, Y.; Shi, J. A core/satellite multifunctional nanotheranostic for *in vivo* imaging and tumor eradication by radiation/photothermal synergistic therapy. *J. Am. Chem. Soc.* **2013**, *135*, 13041–13048. doi:10.1021/ja404985w.
- [487200](#). Liu, B.; Li, C.; Ma, P.; Chen, Y.; Zhang, Y.; Hou, Z.; Huang, S.; Lin, J. Multifunctional NaYF₄:Yb, Er@mSiO₂@Fe₃O₄-PEG nanoparticles for UCL/MR bioimaging and magnetically targeted drug delivery. *Nanoscale* **2015**, *7*, 1839–1848. doi:10.1039/C4NR05342G.

